# Performance of different modelling approaches for the simulation of pile driving process and for the estimation of the dynamic foundation-subsoil interaction of a wind turbine

Dr.-Ing. Stylianos Chrisopoulos

September 2021
Patras

# Content

i. **FE model for the simulation of the vibratory pile installation technique in saturated soils**

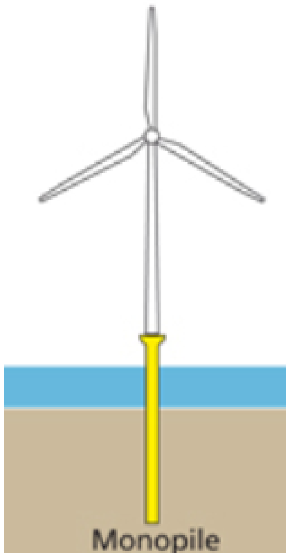


ii. **Development of an engineer-oriented model for monopile foundations based on the HCA model**

iii. **Estimation of the dynamic foundation-subsoil interaction of a wind turbine**

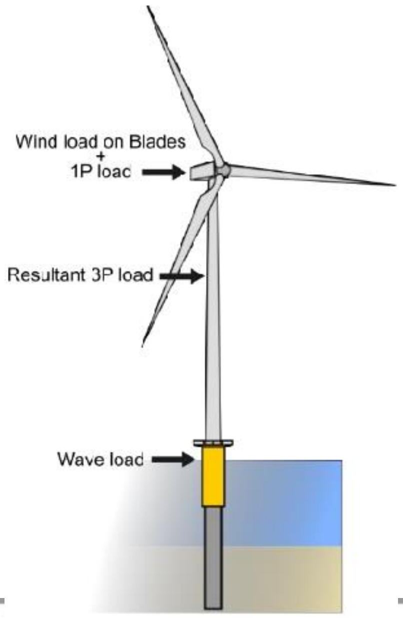


[The cyclic loads acting on the offshore wind turbine structure]

# i. FE model for the simulation of the vibratory pile installation technique in saturated soils

# Motivation

<u>Vibratory pile driving in saturated soil</u>

- Deformations in the surrounding soil
- Stress redistributions (Decrease of effective stresses)
- Large displacements of adjacent structures

(Aubram et al., 2015)

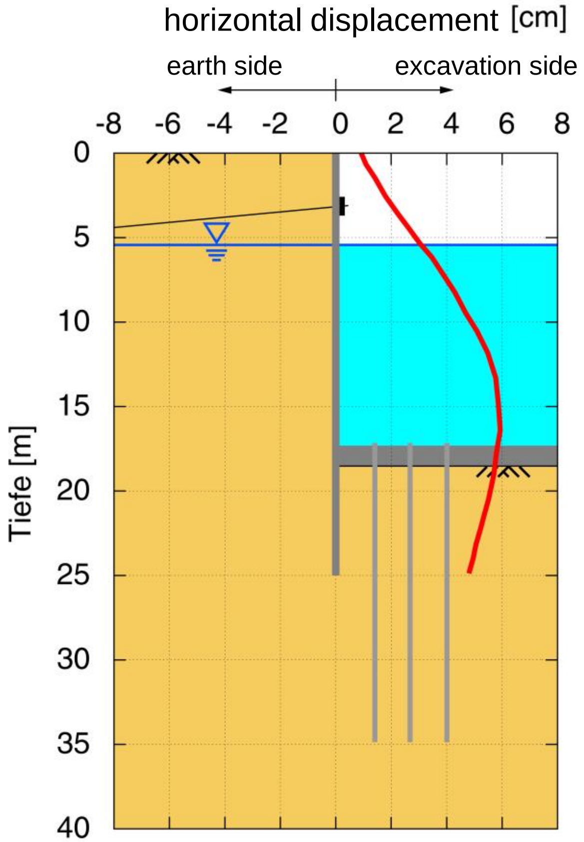


(Triantafyllidis, 1998)

# Motivation

Demand:
Development of a reliable modelling approach for the simulation of soil deformation and stress redistribution during vibratory pile installation process in water-saturated soil

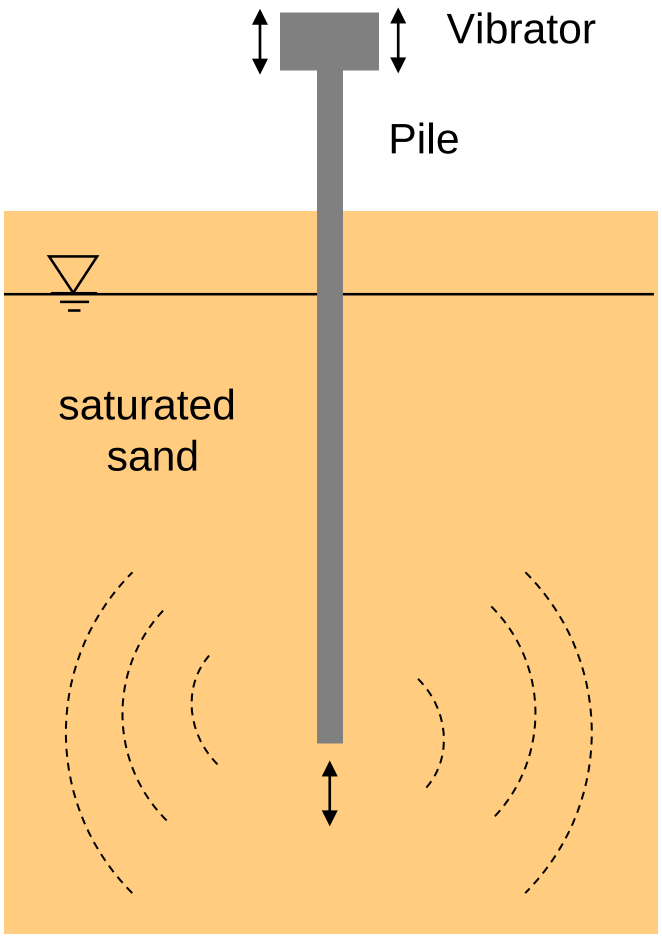


Difficulties:

- Interaction problem with large material deformations
- Dynamic problem in water-saturated soil
- High requirements for suitable constitutive models due to cyclic deformation process

  - Only few studies in the literature
  - No validation with experimental data

# Methodology

- Development and implementation of a user-defined element in Abaqus/Standard for the dynamic analysis of fluid-saturated soils
- Establishing of FE models for the simulation of vibratory pile driving
- Quantitative verification of the numerical modelling approaches based on comparisons with model tests for vibratory pile driving
- Investigation of whether the FE models can reproduce the essential aspects of vibratory pile driving

# Theory of Porous Media

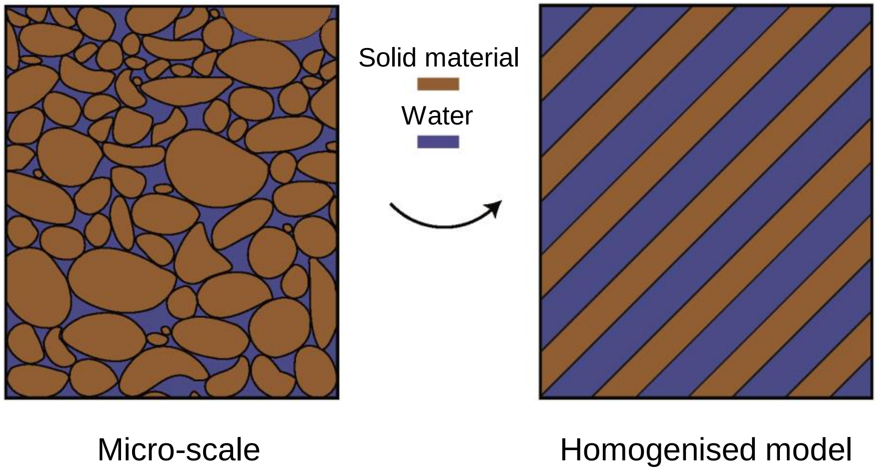


- Constituents are present as continuous phases
- Considering as a homogenised continuum
- **u**-*p*-approximation for a two-phase medium (Zienkiewicz, 1983)
- Axisymmetric 2D-formulation

# Strong form of the equations
## (**u**-*p*-Approximation)

- Equations of motion

$$\operatorname{div}\boldsymbol{\sigma} - \operatorname{grad} p + \varrho\,\mathbf{g} = \varrho\ddot{\mathbf{u}}$$

$$-\operatorname{grad} p + \varrho_f\,\mathbf{g} - \frac{1}{k}\,\varrho_f\,g\mathbf{w} = \varrho_f\,\ddot{\mathbf{u}}$$

- Constitutive equation for the pore pressure

$$\dot{p} = -\frac{K_f}{n}\operatorname{div}\left(\mathbf{w} + \dot{\mathbf{u}}\right)$$

- Constitutive equations for the effective stresses (hypoplasticity with intergranular strain)

# Weak form of the equations

$$\int_\Omega (\operatorname{div}\boldsymbol{\sigma} - \operatorname{grad} p + \varrho\,\mathbf{g} - \varrho\ddot{\mathbf{u}}) \cdot \delta\mathbf{u}\, d\Omega = 0 \quad \Longrightarrow$$

$$\int_\Omega [\boldsymbol{\sigma} : \operatorname{grad}\delta\mathbf{u} - p \operatorname{div}\delta\mathbf{u} + \varrho\,(-\mathbf{g} + \ddot{\mathbf{u}}) \cdot \delta\mathbf{u}]\, d\Omega - \int_{\Gamma_t} \mathbf{t}^{tot} \cdot \delta\mathbf{u}\, d\Gamma = 0$$

$$\int_\Omega \left[\frac{n}{K_f}\,\dot{p} + \operatorname{div}(\mathbf{w} + \dot{\mathbf{u}})\right] \delta p\, d\Omega = 0 \quad \Longrightarrow$$

$$\int_\Omega \left[\left(\frac{n}{K_f}\,\dot{p} + \operatorname{div}\dot{\mathbf{u}}\right)\delta p + \frac{k}{g}\left(\frac{1}{\varrho_f}\operatorname{grad} p - \mathbf{g} + \ddot{\mathbf{u}}\right) \cdot \operatorname{grad}\delta p\right] d\Omega$$
$$- \int_{\Gamma_q} q\, \delta p\, d\Gamma = 0$$

DAAD Deutscher Akademischer Austausch Dienst German Academic Exchange Service
KIT Karlsruhe Institute of Technology
UNIVERSITY OF PATRAS

# Spatial discretisation

- Taylor-Hood-formulation

$$\mathbf{u} = N_I^u \mathbf{u}_I, \quad p = N_J^p p_J$$

$$\delta\mathbf{u} = N_I^u \delta\mathbf{u}_I, \quad \delta p = N_J^p \delta p_J$$

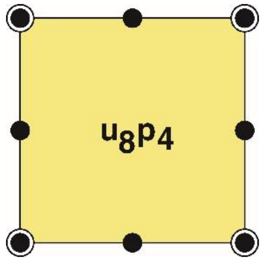


- System for the nodal variables $\mathbf{u}_I$, $p_J$ and their time derivatives:

$$\int_\Omega (\boldsymbol{\sigma} \cdot \operatorname{grad} N_I^u - \varrho N_I^u \mathbf{g})\, d\Omega - p_J \int_\Omega N_J^p \operatorname{grad} N_I^u \, d\Omega$$
$$+ \ddot{\mathbf{u}}_K \int_\Omega \varrho N_I^u N_K^u d\Omega - \int_{\Gamma_t} \mathbf{t}^{tot} N_I^u d\Gamma = 0$$

$$\dot{p}_L \int_\Omega \frac{n}{K_f} N_L^p N_J^p d\Omega + \dot{\mathbf{u}}_K \cdot \int_\Omega N_J^p \operatorname{grad} N_K^u \, d\Omega$$
$$+ p_L \int_\Omega \frac{k}{g \varrho_f} \operatorname{grad} N_L^p \cdot \operatorname{grad} N_J^p \, d\Omega - \int_\Omega \frac{k}{g} \mathbf{g} \cdot \operatorname{grad} N_J^p \, d\Omega$$
$$+ \ddot{\mathbf{u}}_I \cdot \int_\Omega \frac{k}{g} N_I^u \operatorname{grad} N_J^p \, d\Omega - \int_{\Gamma_q} q N_J^p d\Gamma = 0$$

# Time integration + solution process

$$\mathbf{M}\ddot{\mathbf{d}} - \mathbf{G}\left(\mathbf{d}, \dot{\mathbf{d}}\right) = \mathbf{0} \qquad \text{with} \quad \mathbf{d} = \{\mathbf{u}_I, p_J\}$$

$$\mathbf{M}\ddot{\mathbf{d}}_{(t+\Delta t)} - \mathbf{G}\left(\mathbf{d}_{(t+\Delta t)}, \dot{\mathbf{d}}_{(t+\Delta t)}\right) = \mathbf{F}\left(\mathbf{d}_{(t+\Delta t)}, \dot{\mathbf{d}}_{(t+\Delta t)}, \ddot{\mathbf{d}}_{(t+\Delta t)}\right) = \mathbf{0}$$

HILBER – HUGHES – TAYLOR

$$\ddot{\mathbf{d}}_{(t+\Delta t)} = \mathbf{f}_1\left(\mathbf{d}_{(t+\Delta t)}, \mathbf{d}_{(t)}, \dot{\mathbf{d}}_{(t)}, \ddot{\mathbf{d}}_{(t)}\right)$$

$$\dot{\mathbf{d}}_{(t+\Delta t)} = \mathbf{f}_2\left(\mathbf{d}_{(t+\Delta t)}, \mathbf{d}_{(t)}, \dot{\mathbf{d}}_{(t)}, \ddot{\mathbf{d}}_{(t)}\right)$$

$$\mathbf{F}\left(\mathbf{d}_{(t+\Delta t)}, \mathbf{d}_{(t)}, \dot{\mathbf{d}}_{(t)}, \ddot{\mathbf{d}}_{(t)}\right) = \mathbf{F}\left(\mathbf{d}_{(t+\Delta t)}\right) \stackrel{!}{=} \mathbf{0}$$

NEWTON – RAPHSON

AMATRX

RHS

$$\mathbf{d}^{(i+1)} = \mathbf{d}^{(i)} + \mathbf{c}^{(i+1)} \qquad \boxed{\left[\frac{\partial \mathbf{F}}{\partial \mathbf{d}}\right]^{(i)}} \cdot \{\mathbf{c}\}^{(i+1)} = \boxed{\{-\mathbf{F}\}^{(i)}}$$

# Verification of the user element

- Spherically symmetric problem

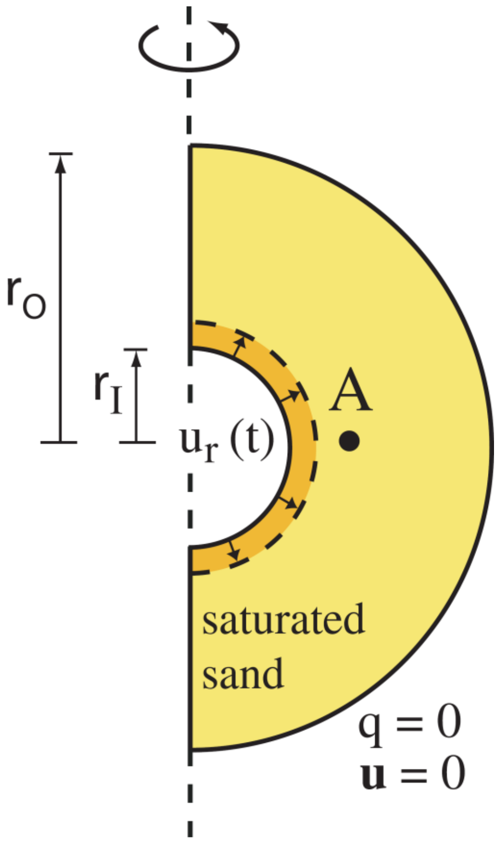


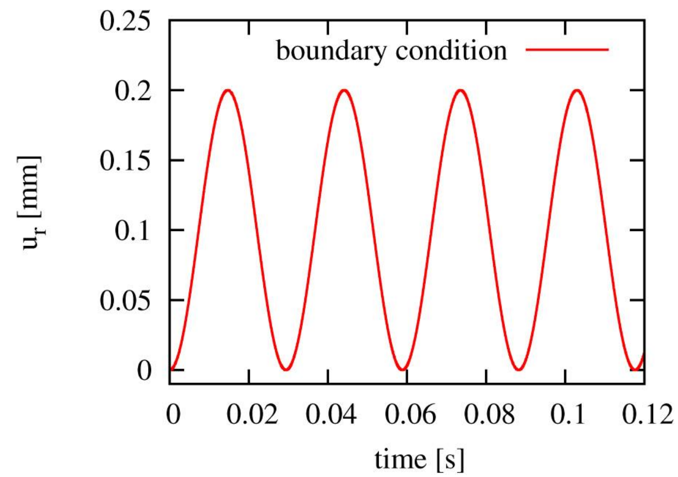


- Verification by the comparison of the finite-element solution (user element) with the 1D finite-difference solution

- Inner radius $r_I$=15 cm
- Outer radius $r_O$=5 m
- Finite element size 1.2 cm to 20 cm
- Impermeable outer boundary with zero displacement
- Vibration frequency 34 Hz

- Hypoplasticity with intergranular strain
- $K_f$ = 100 MPa
- Isotropic initial effective stress -50 kPa
- Pore pressure 50 kPa
- Void ratio 0.6
- Soil permeability $k$=$10^{-3}$ m/sec

# Verification of the user element

- Comparison with 1D spherically symmetric finite-difference solution

Radial and circumferential effective stresses vs. time at Point **A** ($r_A$ = 20 cm)

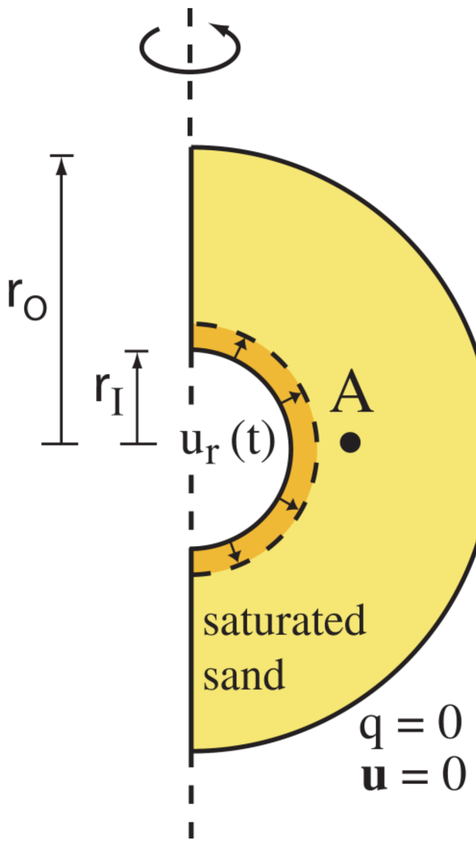


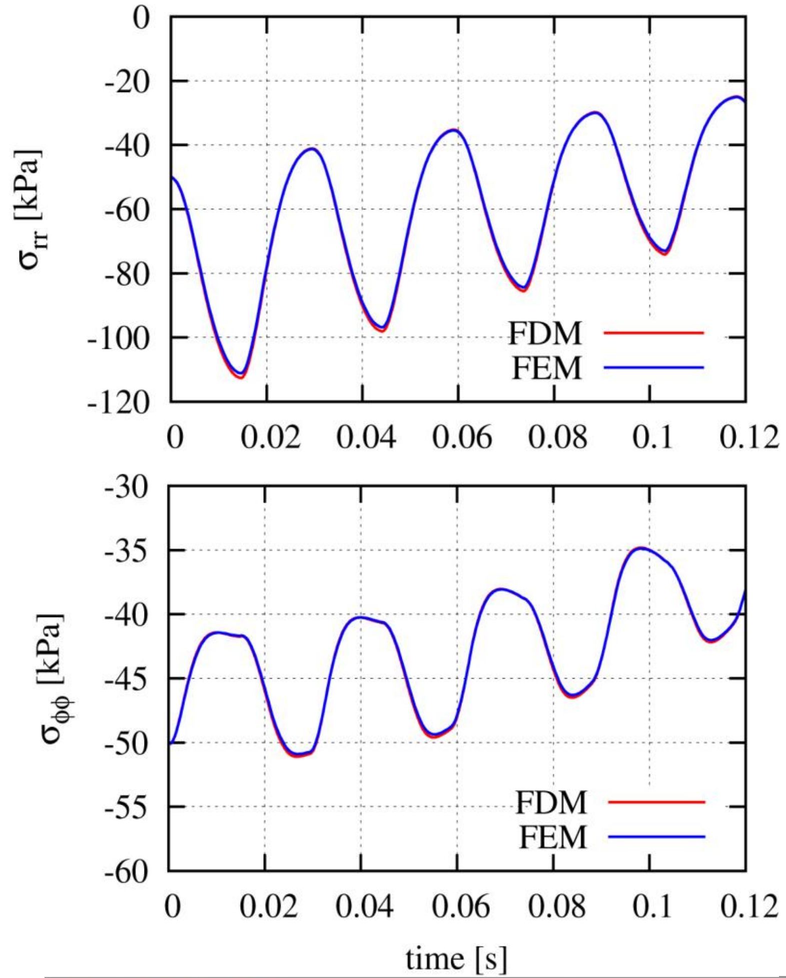

# Geotechnical problem

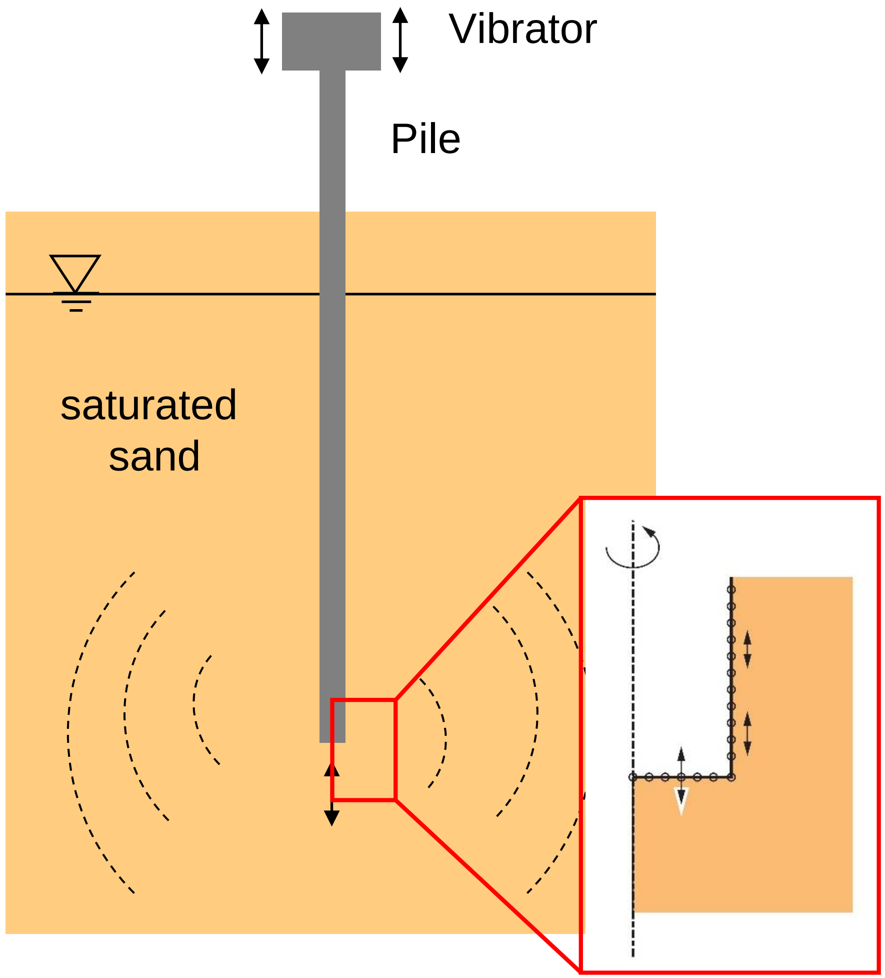


## Simplified Modeling technique:

- Pile not explicitly modeled
- Pile-soil interaction considered through imposed cyclic soil displacements at the interface
- No or very low penetration

# Geotechnical problem

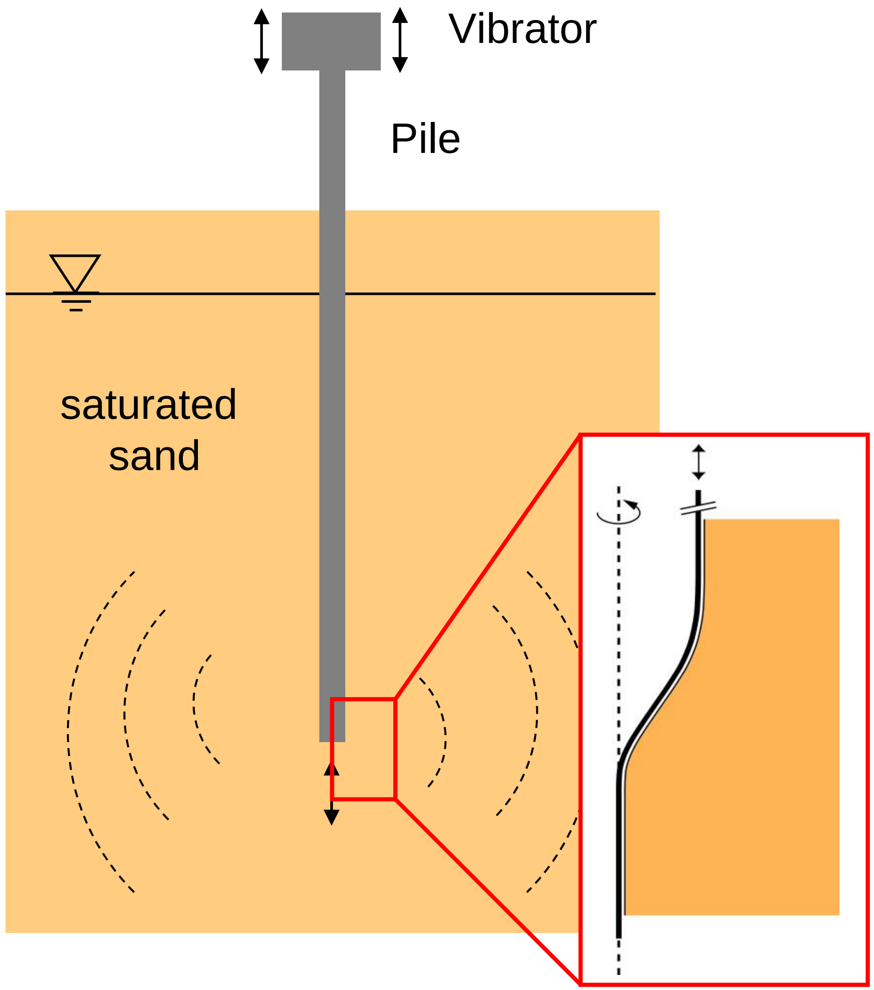


## Enhanced modeling technique:

- Pile as rigid body
- Contact definition at pile-soil interface
- zipper-type technique

# Dynamic boundary value problem (simplified model)

*S. Chrisopoulos, V.A. Osinov, T. Triantafyllidis (2016): Dynamic problem for the deformation of saturated soil in the vicinity of a vibrating pile toe. Lect. Notes Appl. Comput. Mech., 80:53–67*

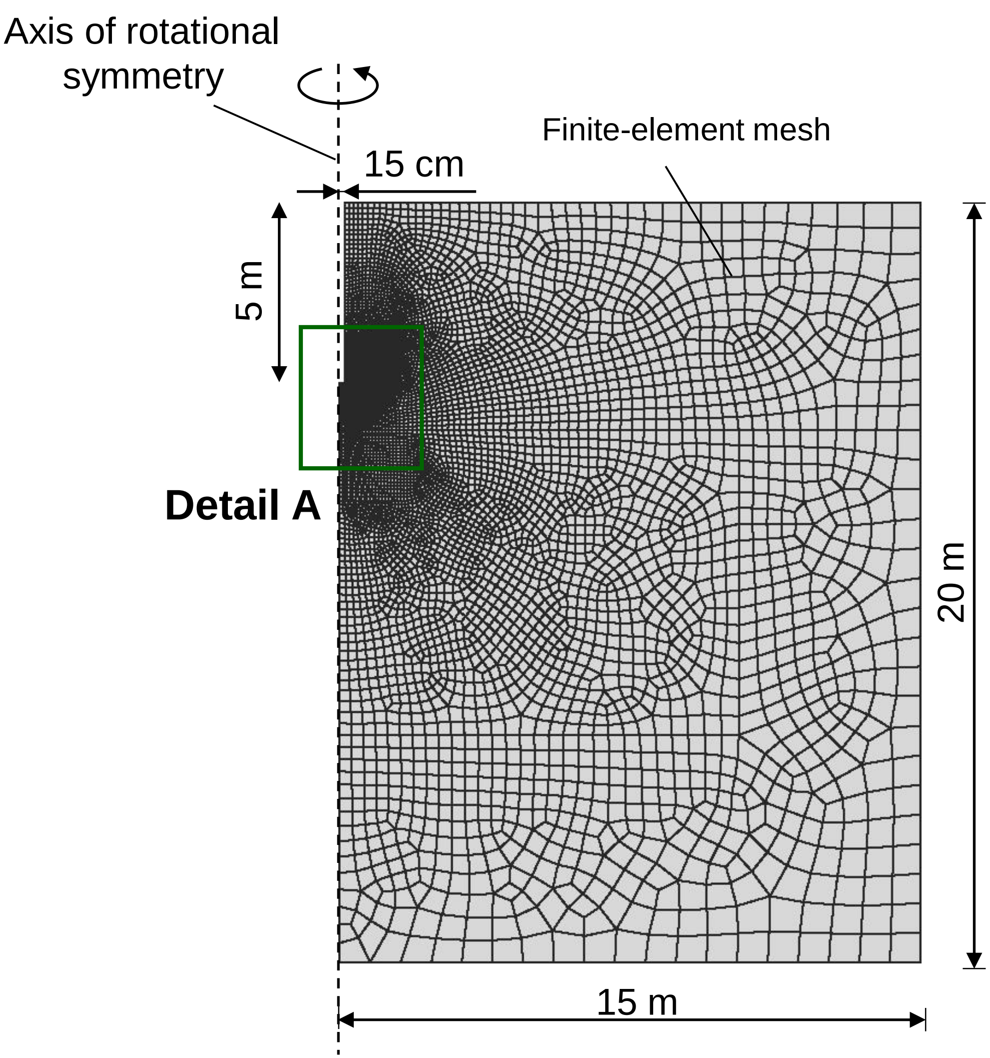


- 2D axisymmetric formulation
- Hypoplasticity with intergranular strain (Karlsruher Sand)
- Full saturated soil ($K_f$ = 2.2 GPa)
- Geostatic initial effect. stress ($K_0$ =1)
- Void ratio 0.6 (dense)
- Soil permeability:
  - $k$ = 0 m/s (local undrained)
  - $k$ = $10^{-4}$ ,$10^{-3}$ m/s (local drained)
- Vibration frequency 34 Hz
- $\Delta t$ = $10^{-4}$ s (Period/$\Delta t$ ≈ 300)

# Dynamic boundary value problem (simplified model)

*S. Chrisopoulos, V.A. Osinov, T. Triantafyllidis (2016): Dynamic problem for the deformation of saturated soil in the vicinity of a vibrating pile toe. Lect. Notes Appl. Comput. Mech., 80:53–67*

## Detail A

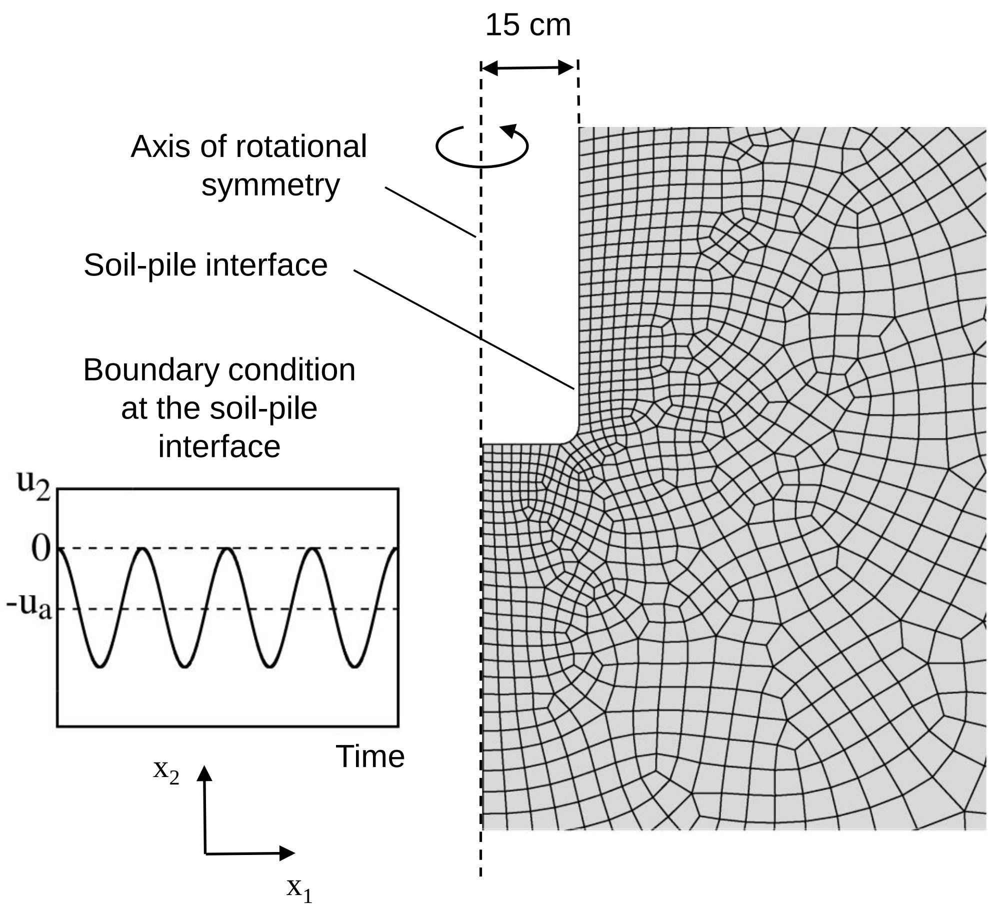


- 2D axisymmetric formulation
- Hypoplasticity with intergranular strain (Karlsruher Sand)
- Full saturated soil ($K_f$ = 2.2 GPa)
- Geostatic initial effect. stress ($K_0$ =1)
- Void ratio 0.6 (dense)
- Soil permeability:
  - $k$ = 0 m/s (local undrained)
  - $k$ = $10^{-4}$ ,$10^{-3}$ m/s (local drained)
- Vibration frequency 34 Hz
- $\Delta t$ = $10^{-4}$ s (Period/$\Delta t$ ≈ 300)

# Numerical solution with locally undrained conditions

**Soil permeability** $k = 0$ m/s

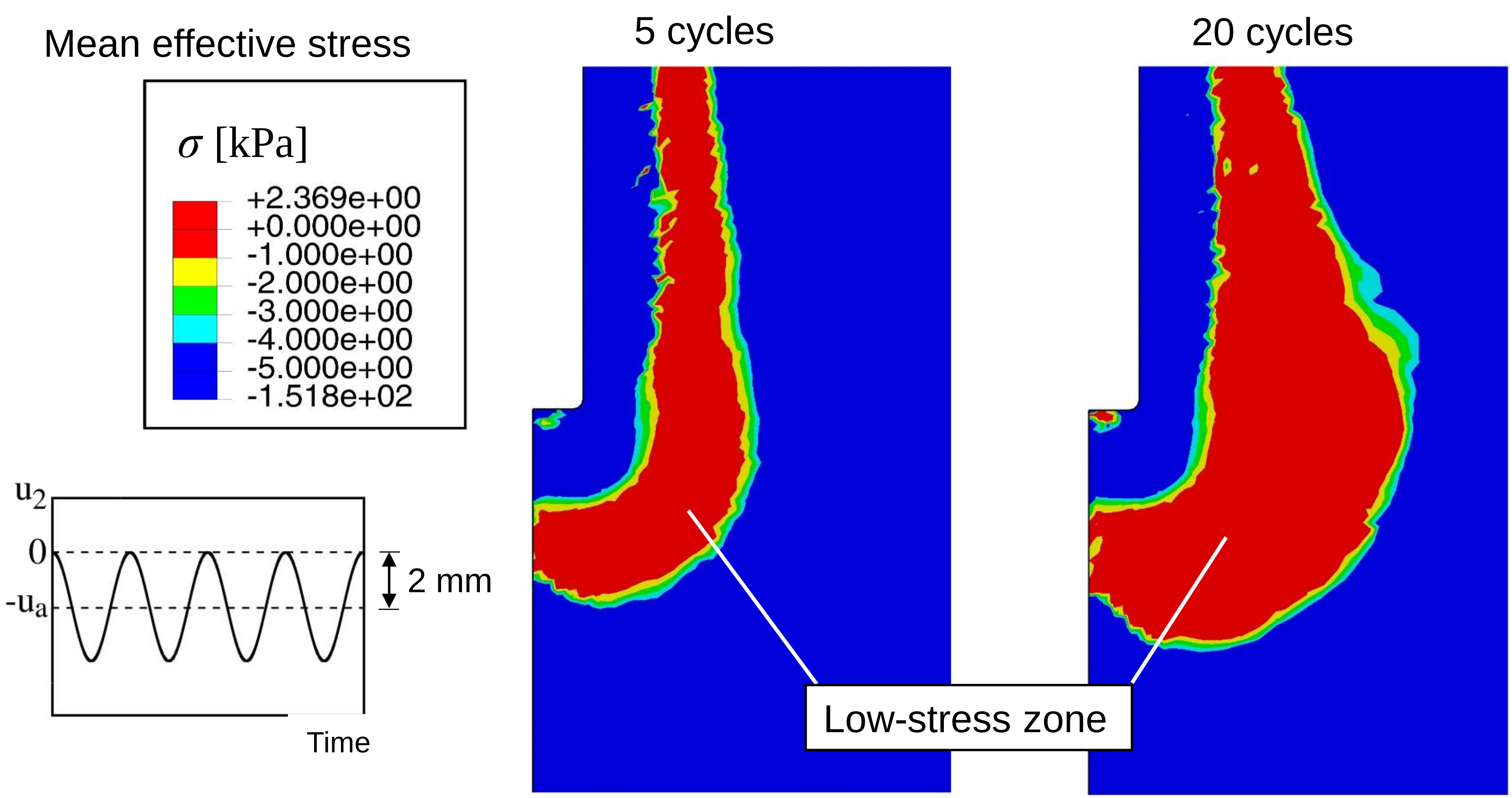


**Result:**

- Formation of a low-stress zone (liquefaction zone) around the pile toe after several cycles of vibration

# Numerical solution with locally drained conditions

**Soil permeability** $k = 10^{-4}$ m/s

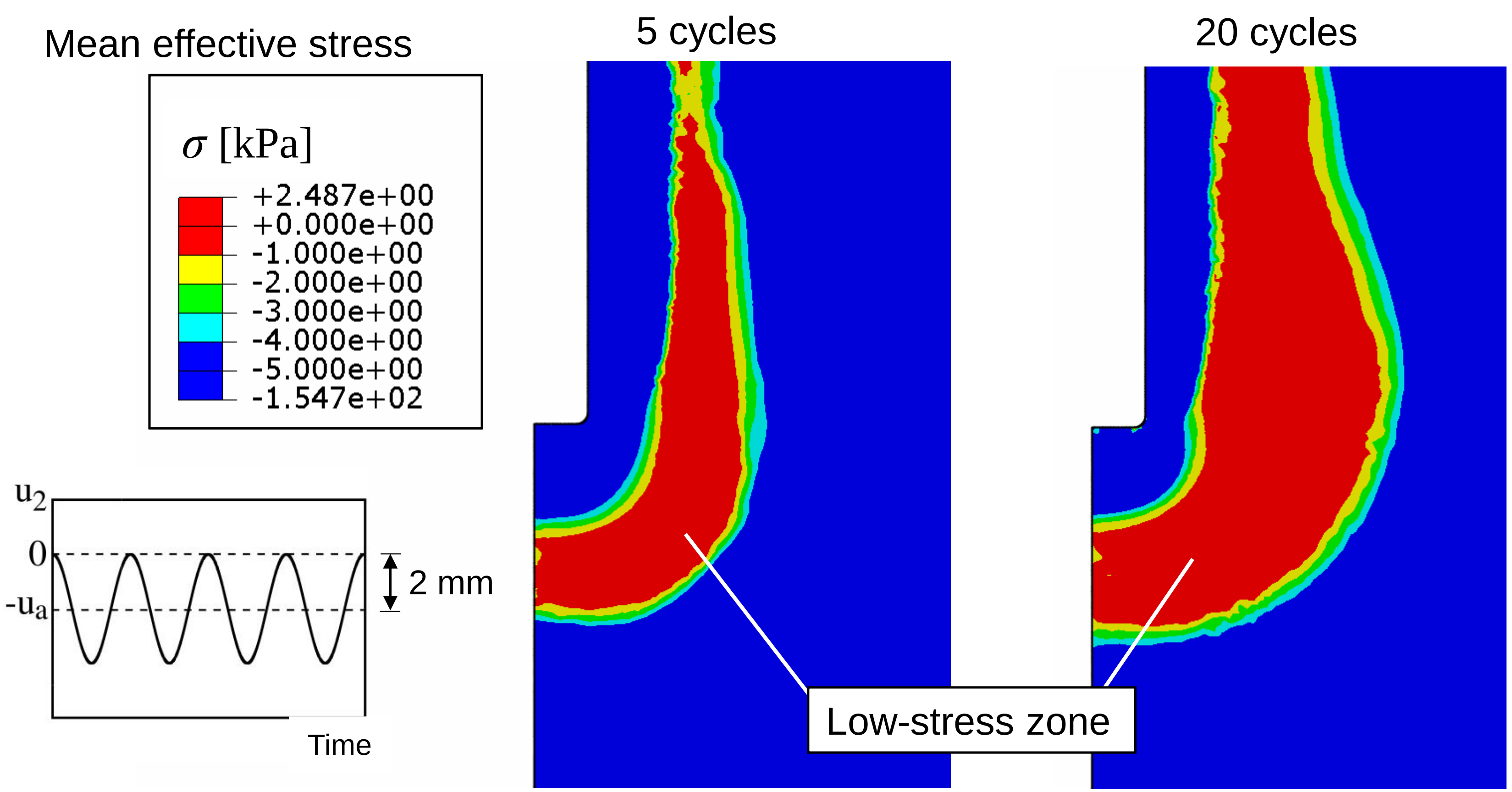

# Numerical solution with locally drained conditions

**Soil permeability** $k = 10^{-3}$ m/s

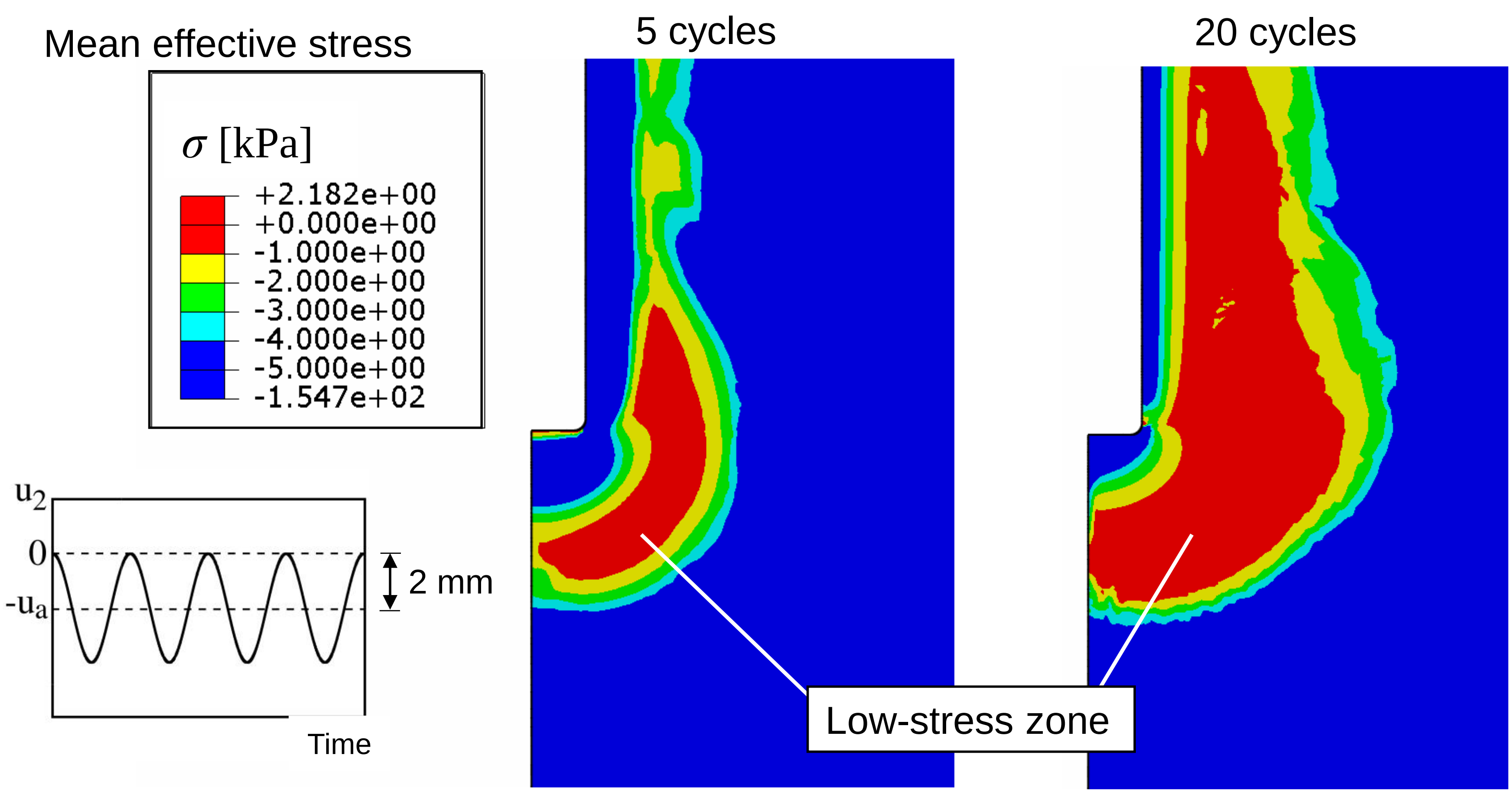


**Result:**

- High permeability do not prevent the formation of a low-stress zone

# Dynamic boundary value problem (enhanced model)

## Detail A

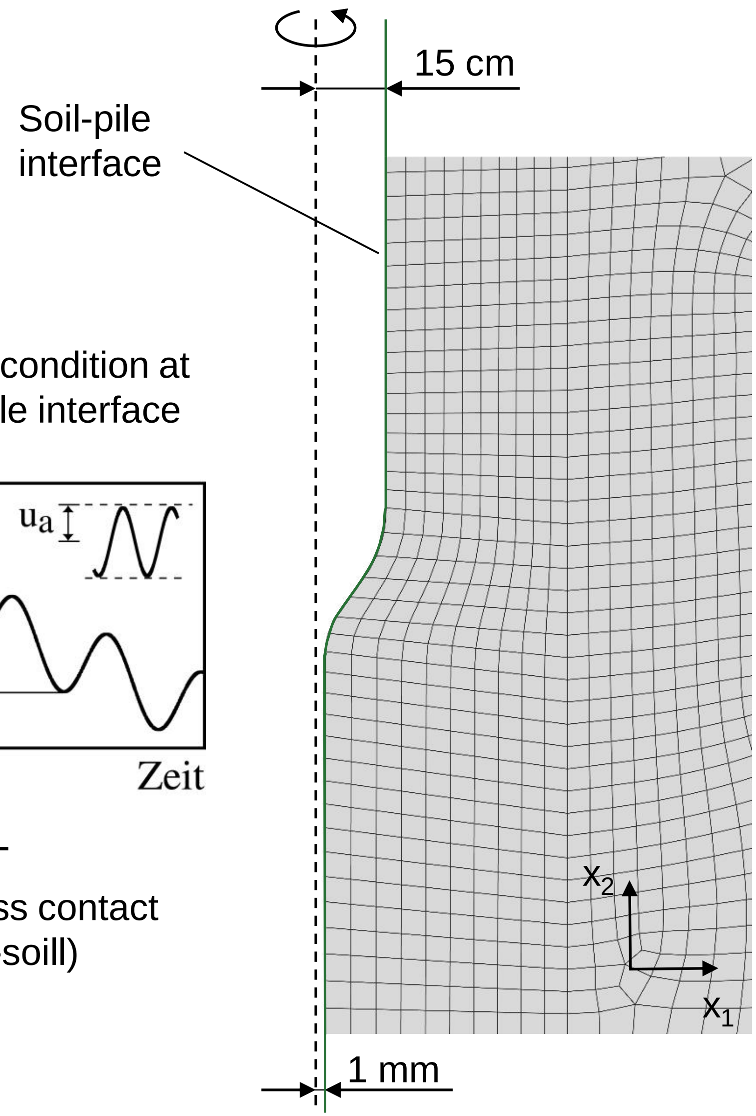


Boundary condition at the soil-pile interface

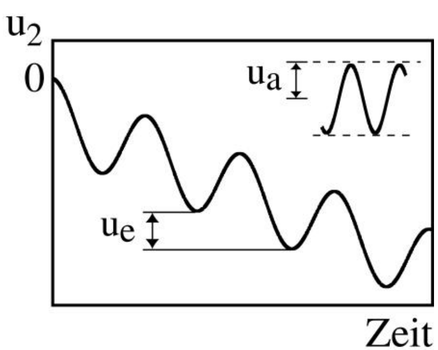


\+

Frictionless contact (pile-soill)

# Numerical solution with locally undrained conditions

## Soil permeability $k$ = 0 m/s

Pore water pressure

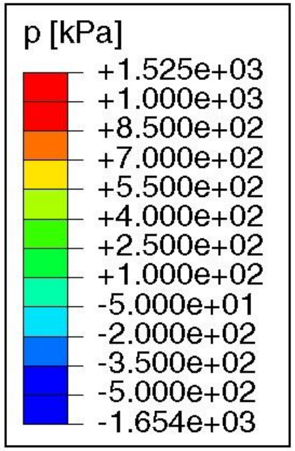


30 cycles

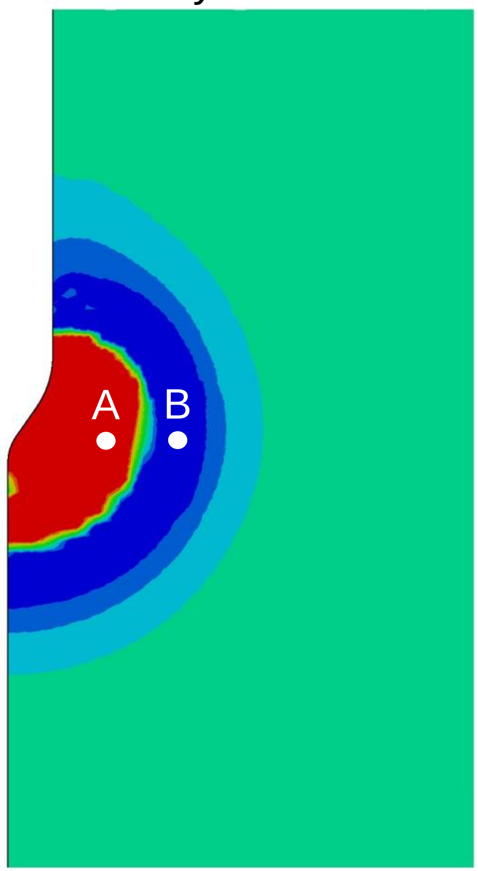


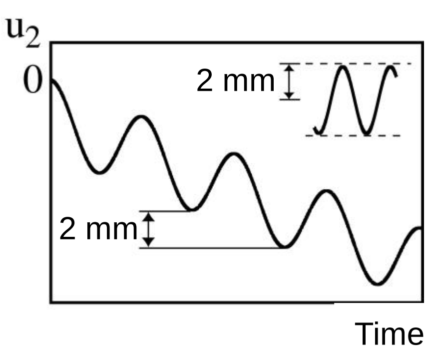


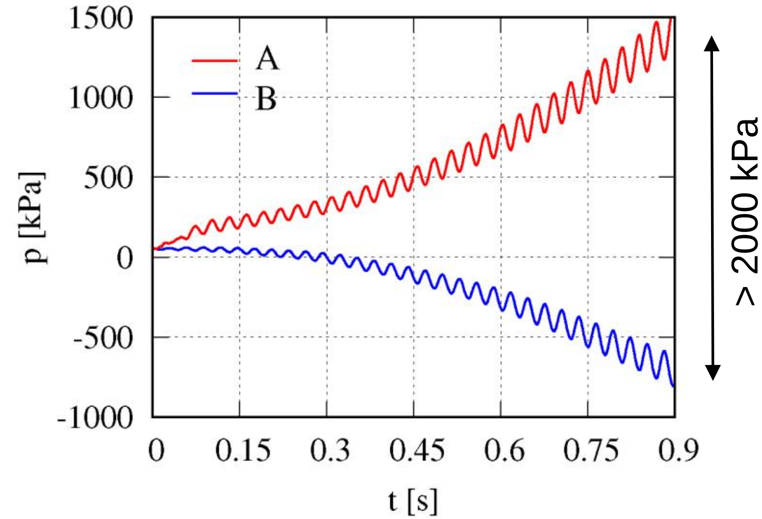


**Result:**

- Very large, unrealistic pore water pressure gradients are created

→ Locally drained conditions are absolutely necessary!

# Numerical solution with locally drained conditions

## Soil permeability $k = 10^{-3}$ m/s

Mean effective stress

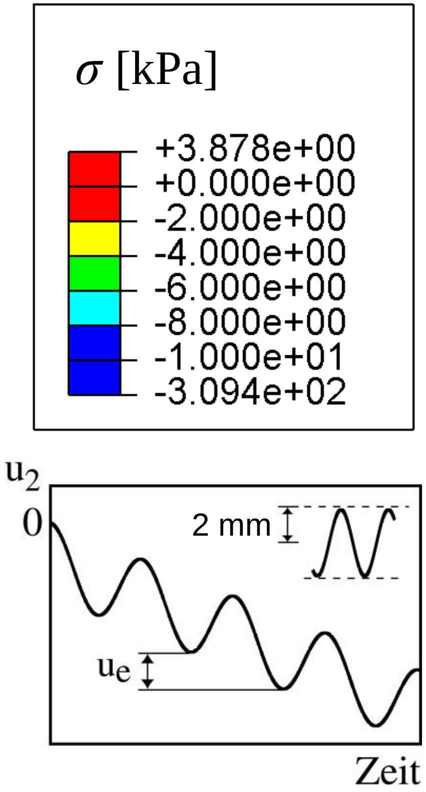


after 50 cycles

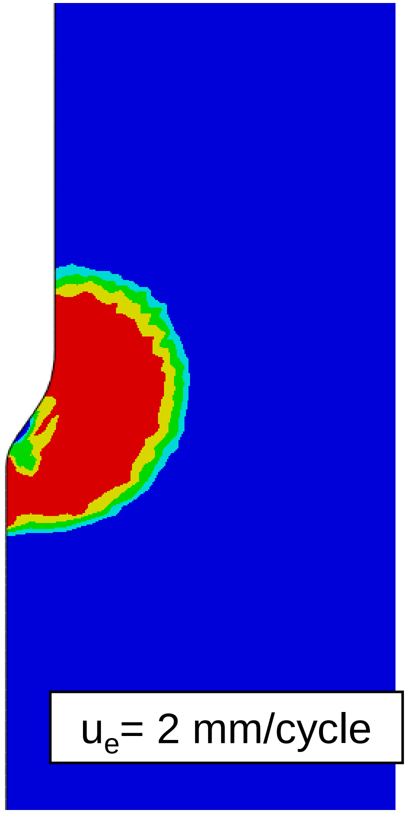


after 50 cycles

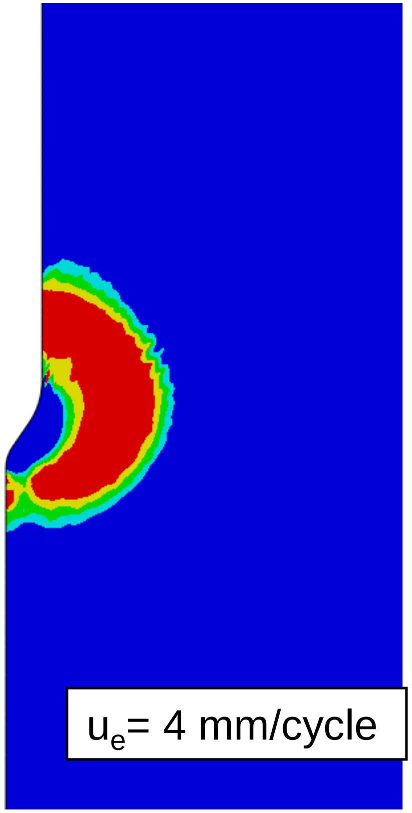


**Result:**

- Despite the monotonic deformation component and the higher permeability, a low-stress zone is formed

# Model test concept

Experimental set-up (Vogelsang, 2017)

- Half-cylinder test device with observation window
- Vibration with 25 Hz for a few seconds

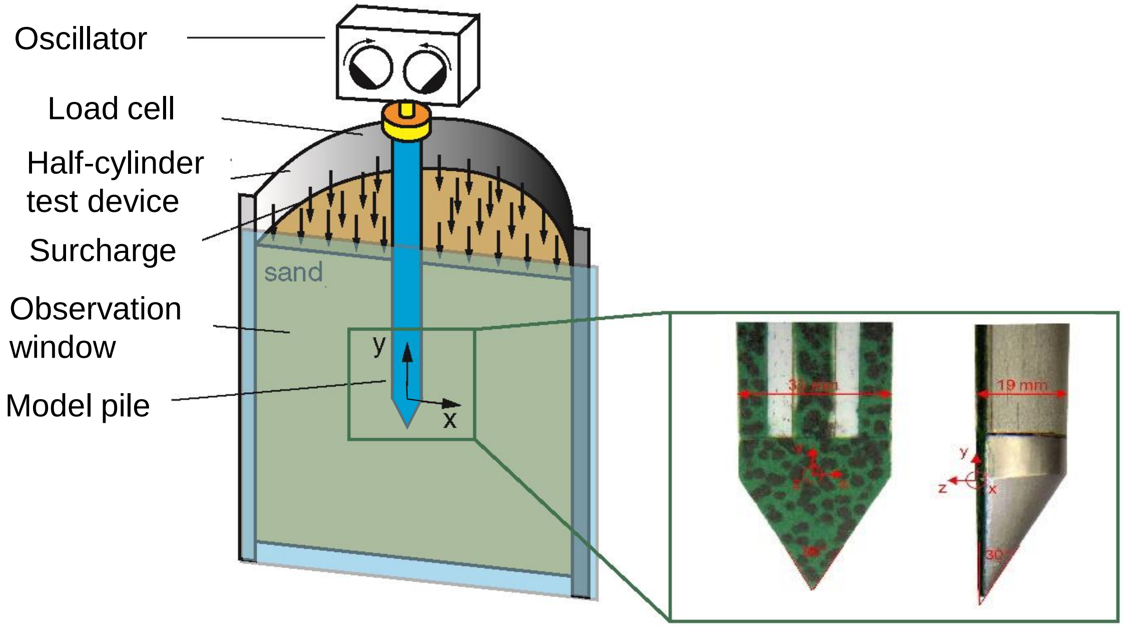

# Model test concept

## Experimental set-up (Vogelsang, 2017)

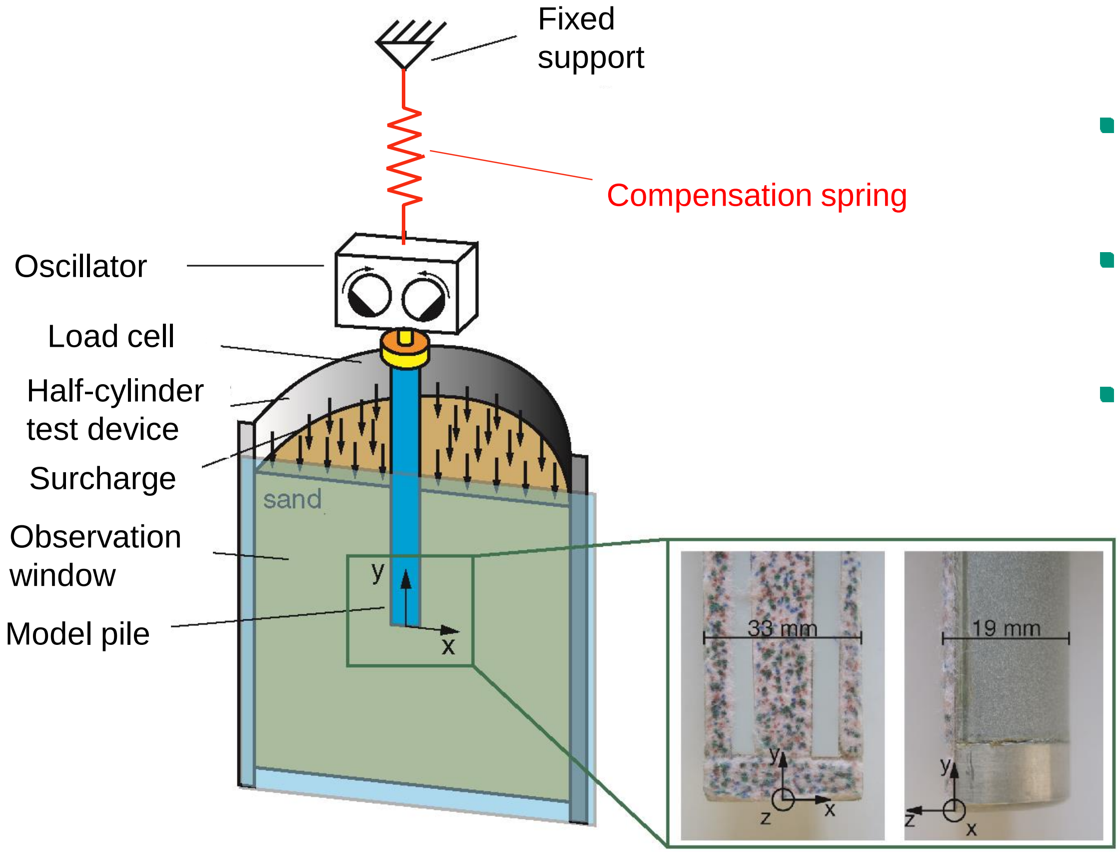


- Half-cylinder test device with observation window
- Vibration with 25 Hz for a few seconds
- Compensation spring minimizes the pile penetration
- Measurements:
  - Soil motion with DIC
  - Pile displacement and pile head force

# Simplified FE-Model

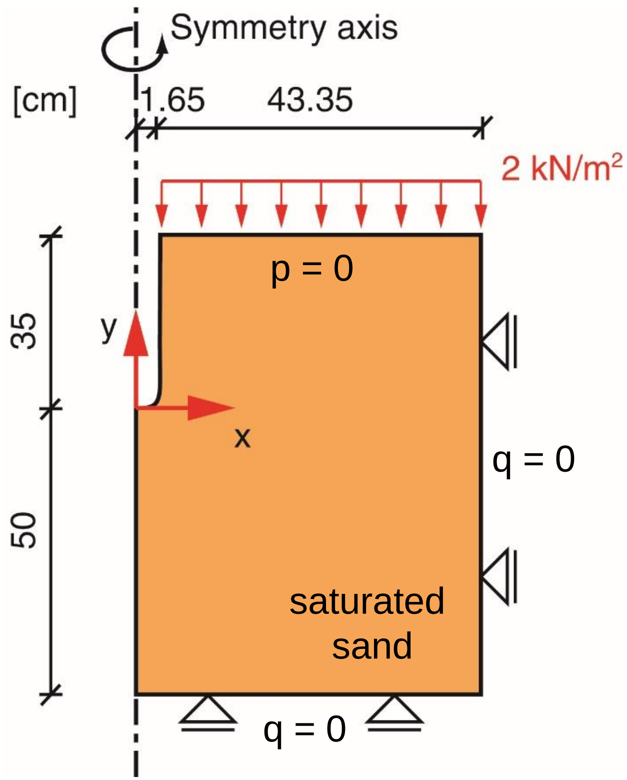


- Full saturation ($K_f$ = 2.2 GPa)
- Geostatic initial effective stress ($K_0$ = 0.4)
- Initial void ratio $e_0$ = 0.72 (medium dense sand)
- Soil permeability:
  - $k = 1.5 \cdot 10^{-3}$ m/s (locally drained)

# Simplified FE-Model

## Modeling of pile-soil interaction

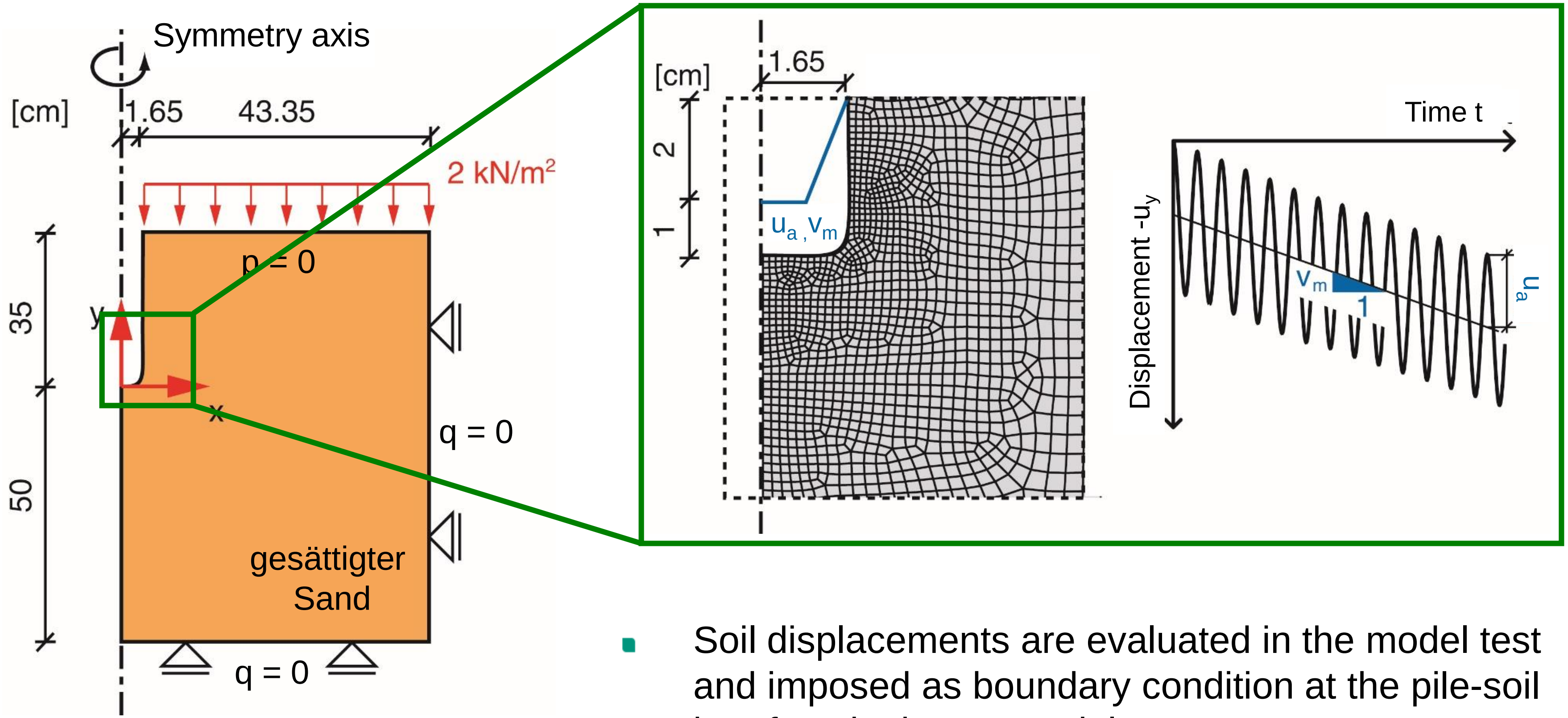


- Soil displacements are evaluated in the model test and imposed as boundary condition at the pile-soil interface in the FE model

# Comparison of FE- and experimental results

## Displacement fields after 25 cycles

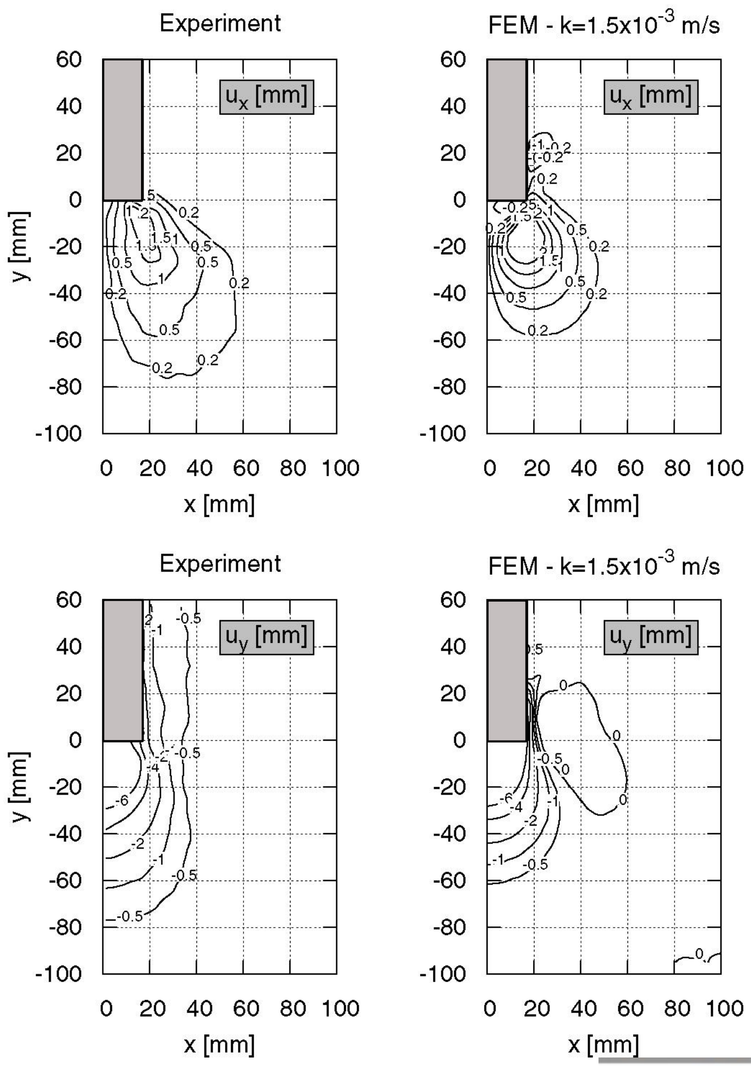


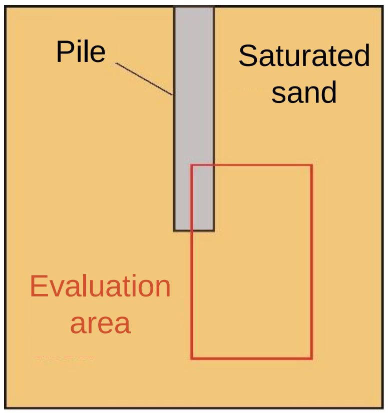


- Simplified model reproduces the soil displacements realistically

# Enhanced FE-Model

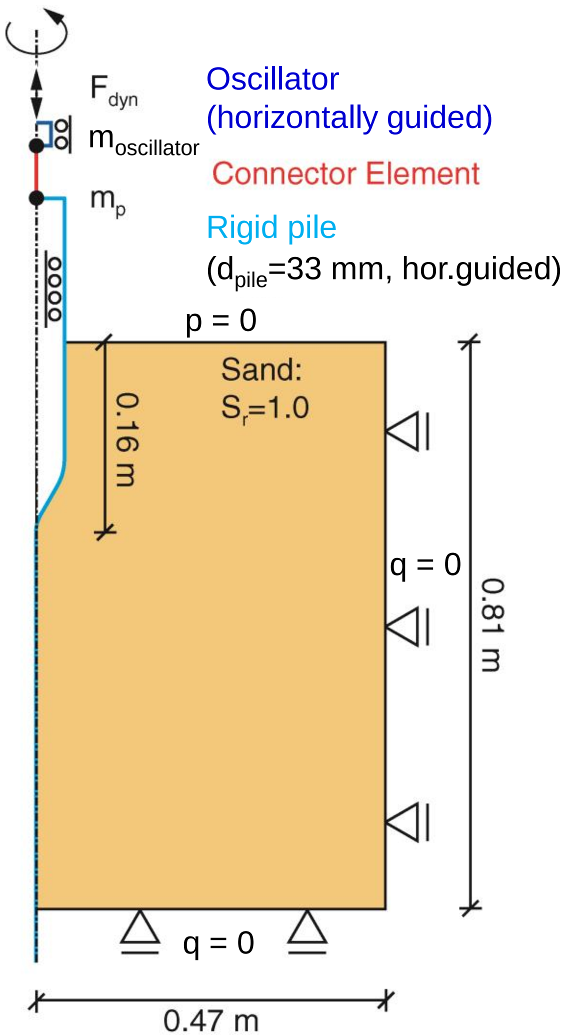


- Oscillator – load cell – pile modeled
- Pile and oscillator rigid bodies
- Frictionless „node-to-surface“ contact between pile-soil
- Initial density und soil permeability
  - $I_{D,0}$ = 0,53 $k = 1.0 \cdot 10^{-3}$ m/s
  - $I_{D,0}$ = 0,71 $k = 1.2 \cdot 10^{-3}$ m/s
  - $I_{D,0}$ = 0,82 $k = 1.4 \cdot 10^{-3}$ m/s

# Enhanced FE-Model

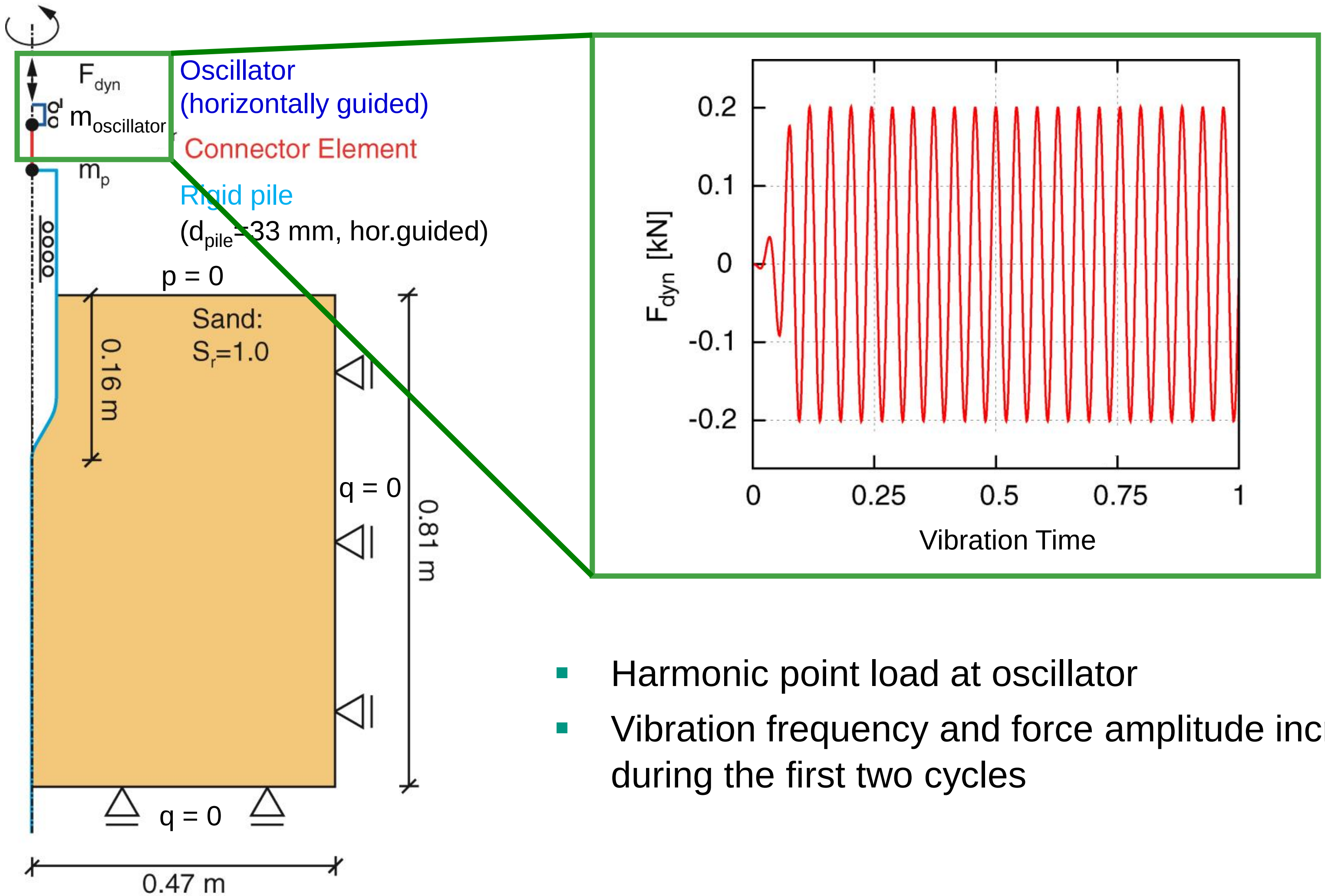


- Harmonic point load at oscillator
- Vibration frequency and force amplitude increase during the first two cycles

# Comparison of FE- and experimental results

Mean penetretion velocity ($v_m$) of pile

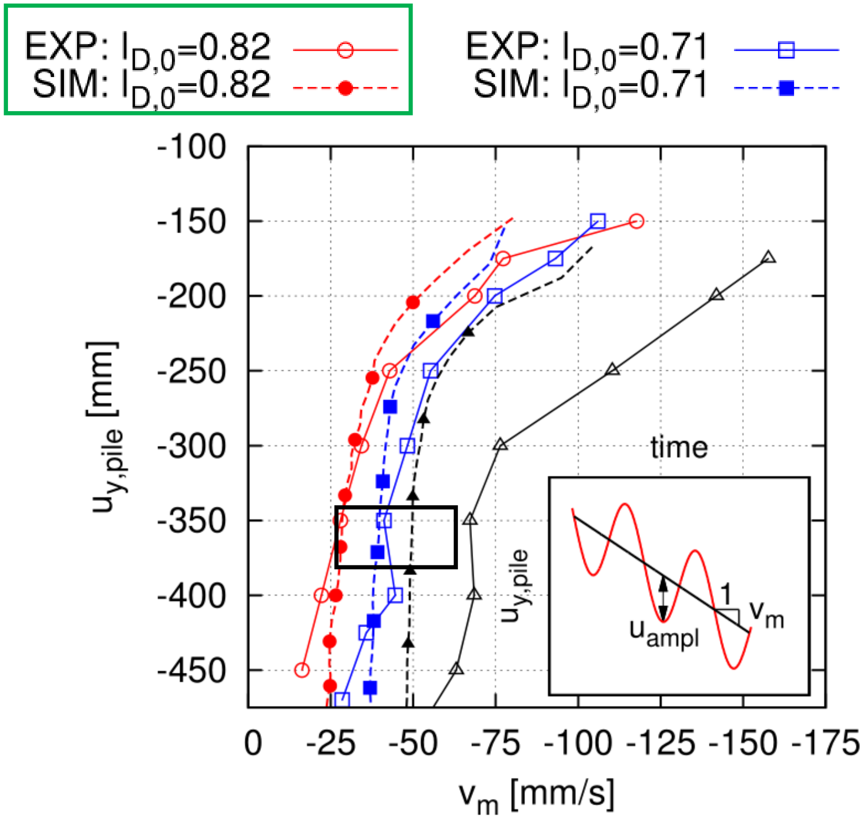


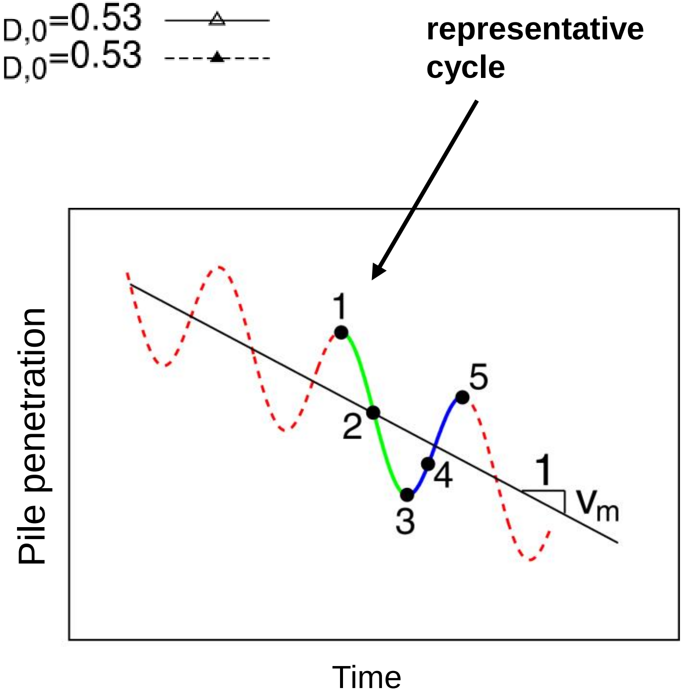


- The mean penetration velocity decreases with depth
- Comparison based on a representative cycle at a depth of about 0.4 m

# Comparison of FE- and experimental results

## Related soil reaction force

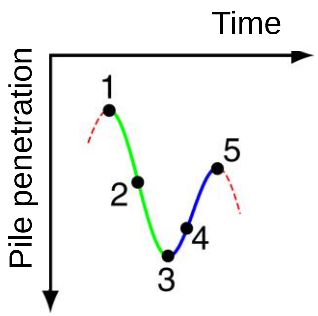


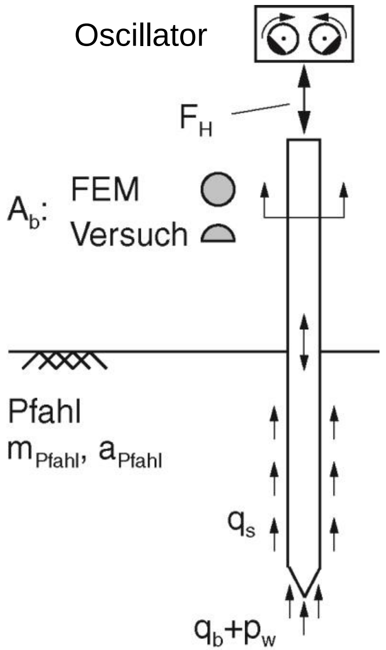


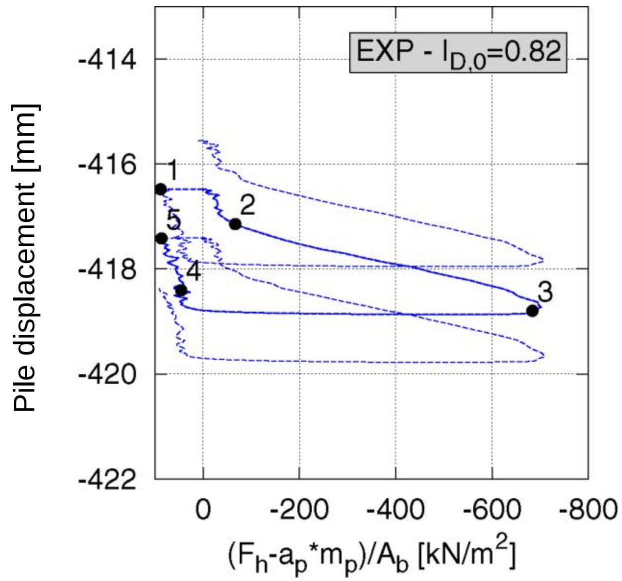


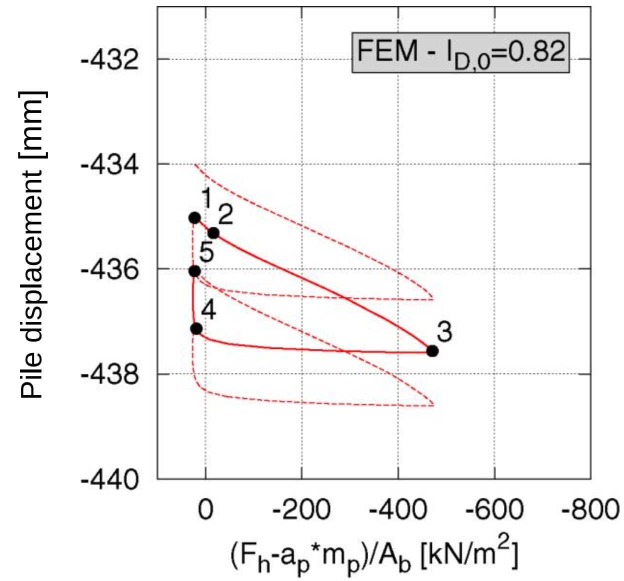


Related soil reaction force: $\dfrac{F_h - m_{Pile} \cdot a_{Pile}}{A_b}$

- Qualitatively similar penetration behaviour
- Lower penetration resistance in the simulation
- Shaft resistance not incorporated in the numerical model

# Comparison of FE- and experimental results

Incremental displacement fields during the penetration phase

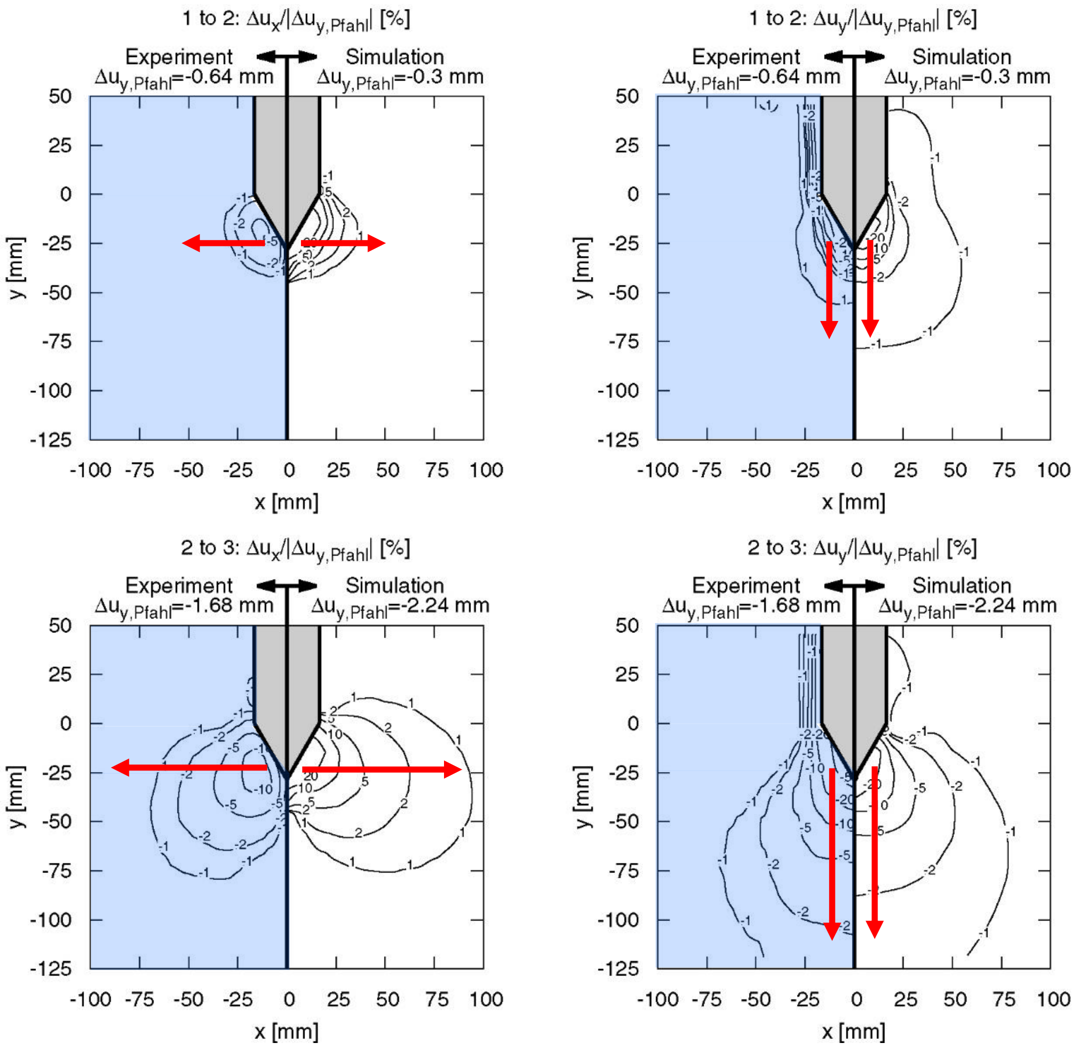


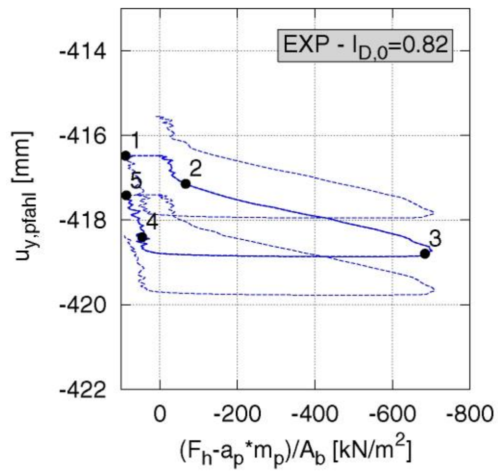


- Phase 1 ÷ 2:
  - Soil displacements in a spherical area of about 1Ø under the pile tip
  - The soil is directed away from the pile
- Phase 2 ÷ 3:
  - Same deformation mechanism to Phase 1 ÷ 2. A deeper and larger zone of the soil is affected

# Comparison of FE- and experimental results

Incremental displacement fields during the upward pile motion

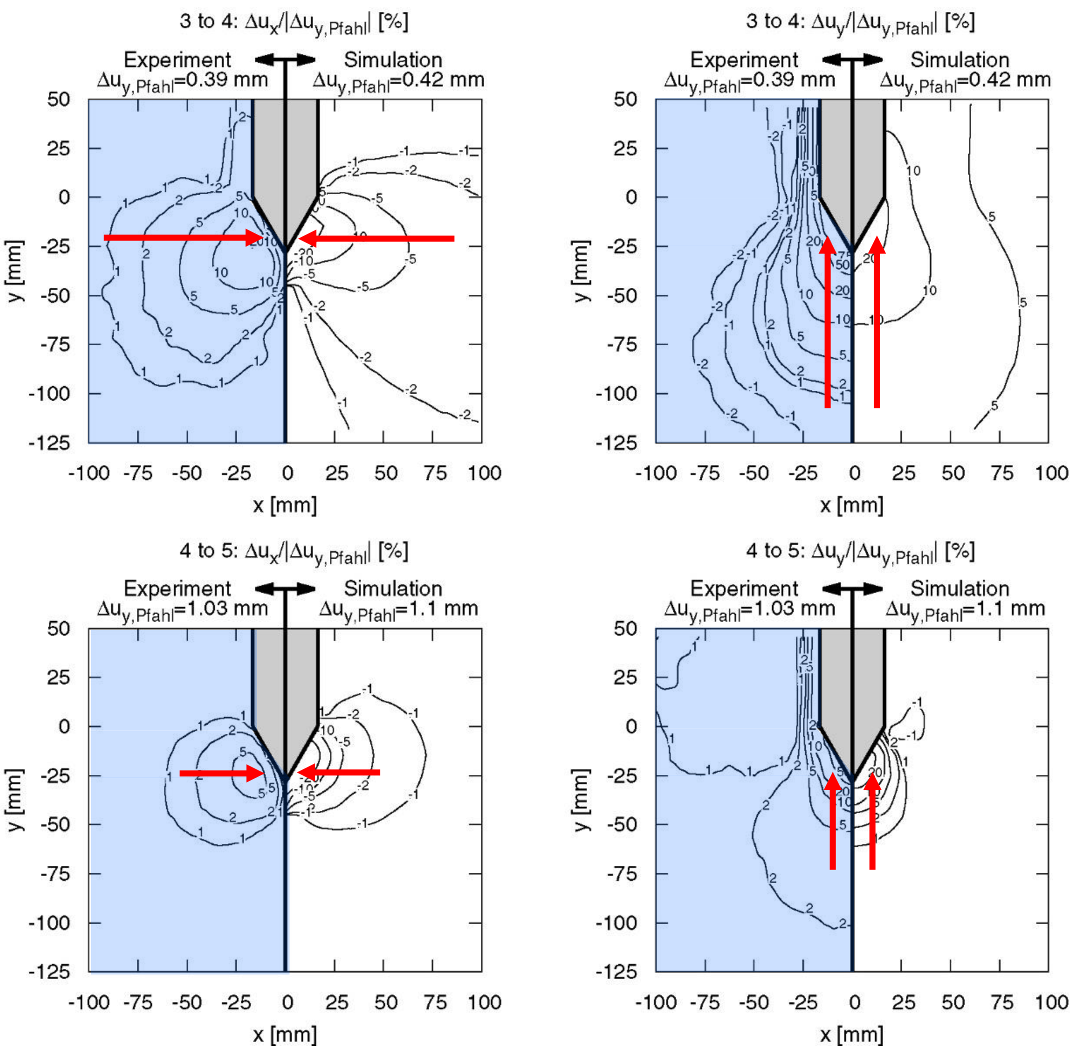


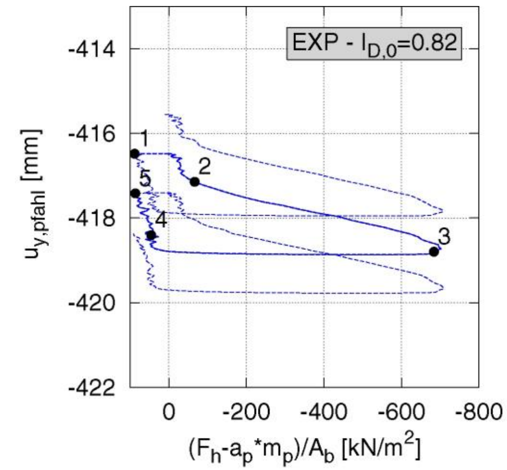


- Phase 3 ÷ 4:
  - The soil is directed to the pile
- Phase 4 ÷ 5:
  - Same deformation mechanism to Phase 3 ÷ 4
  - Soil displacements in a smaller area

*Chrisopoulos & Vogelsang (2019): A finite element benchmark study based on experimental modeling of vibratory pile driving in saturated sand. Soil Dyn. Earthq. Eng., 122:248-260*

# Summary

- A user-defined element was developed and implemented in Abaqus/Standard
- Different FE models were created for the simulation of vibratory pile driving
  - Simplified modeling approach: pile is replaced by a displacement boundary condition.
  - Enhanced modeling approach: pile as rigid body
- Vibratory pile driving in saturated soil results in a zone of nearly zero effective stresses (liquefaction zone) around the pile
- The comparison with model tests for vibratory pile driving confirms that the proposed modeling approaches are able to accurately reproduce the essential aspects of the mechanism of vibratory pile driving.



DAAD Deutscher Akademischer Austausch Dienst German Academic Exchange Service
KIT Karlsruhe Institute of Technology
UNIVERSITY OF PATRAS

# ii. Development of an engineer-oriented model for monopile foundations based on the HCA model

# Engineer-oriented model

Model schema with springs and dashpots arranged on both sides of the beam

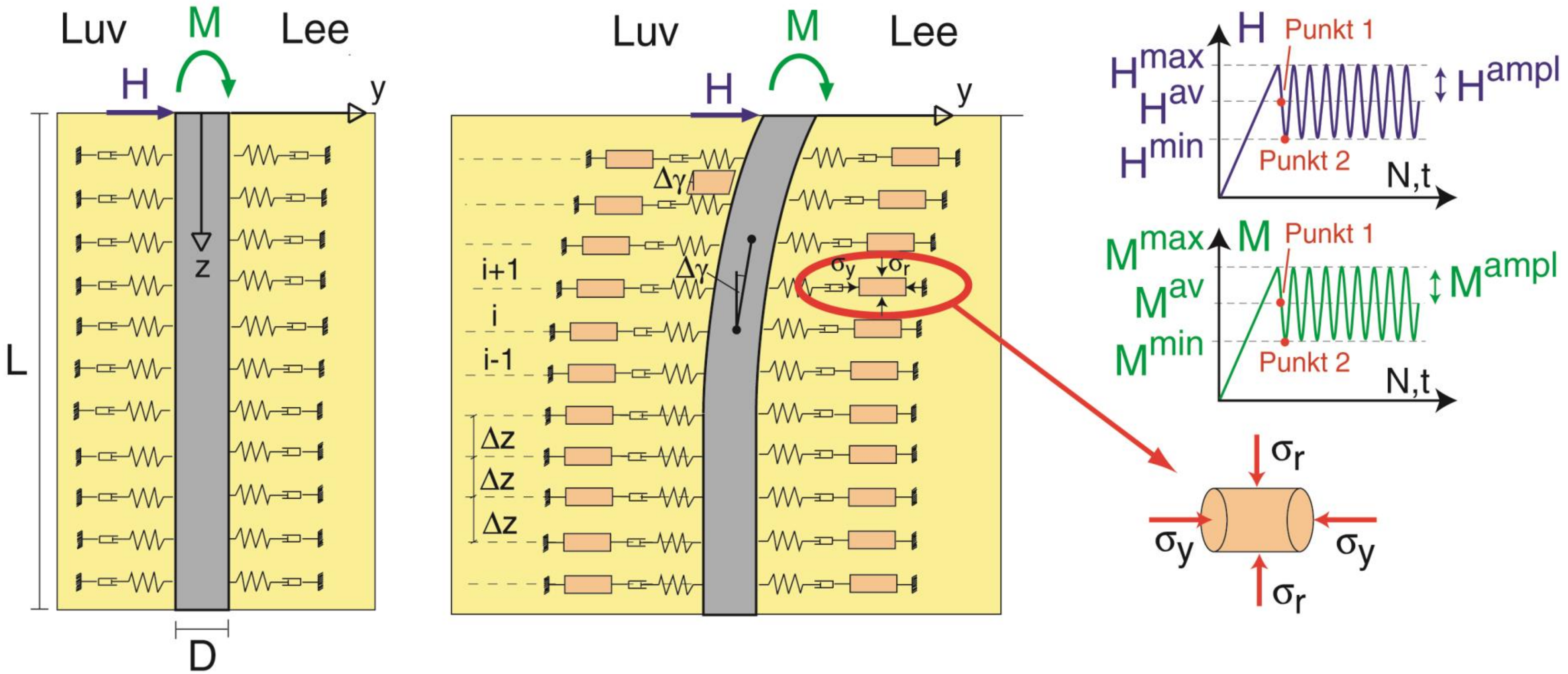


*Triantafyllidis & Chrisopoulos (2016)*

## Engineer-oriented model

Model schema with springs and dashpots arranged only on one side of the beam

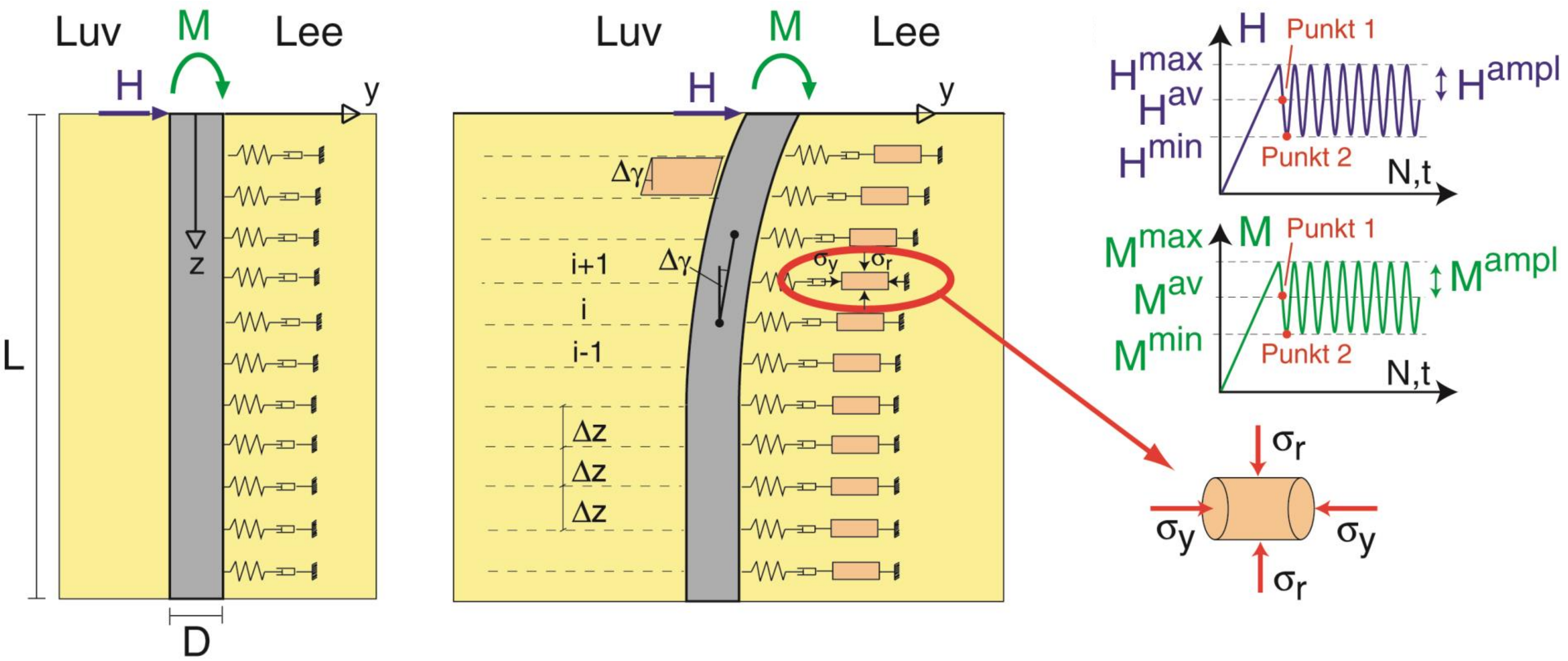


*Triantafyllidis & Chrisopoulos (2016)*

# Engineer-oriented model

## Static loading

Fourth-order differential equation of the beam-on-elastic foundation problem

$$EI \cdot \frac{d^4 y}{dz^4} + K_s(z) \cdot y \cdot D = 0$$

Betting modulus $K_s$ =M/D

where: $M = ((1+e_0)/C_c)\sigma'_y$ for loading

$M = ((1+e_0)/C_s)\sigma'_y$ for unloading

$C_c$: compression index

$C_s$: swelling index

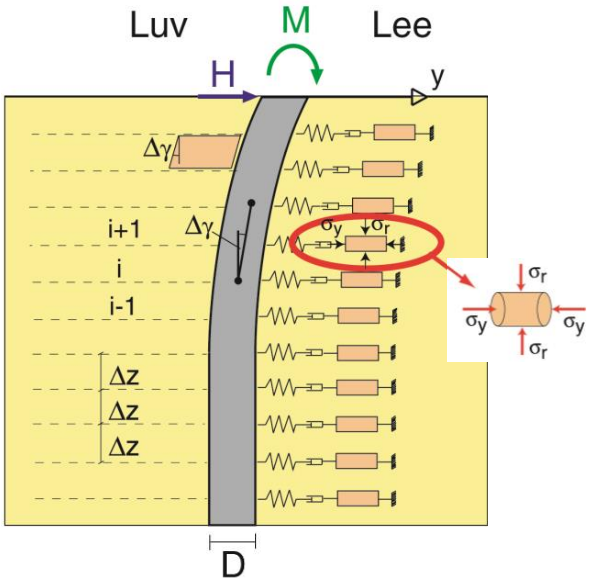


Boundary conditions

At head : z=0

$$EI \cdot \frac{d^2 y}{dz^2} = M_b \qquad EI \cdot \frac{d^3 y}{dz^3} = H$$

At toe : z=L

$$EI \cdot \frac{d^2 y}{dz^2} = 0 \qquad EI \cdot \frac{d^3 y}{dz^3} = 0$$

# Engineer-oriented model

## Cyclic loading

The deformations due to the cyclic loading are treated with equations based on the high-cycle accumulation (HCA) model. The increment of horizontal displacement $\Delta y_i^{\mathrm{Pile}}$ of the pile is coupled with the unknown increment of stress $\Delta\sigma_i$ in the soil caused by the cycles via:

$$[\mathbf{K}]\cdot\left[\Delta y_i^{\mathrm{Pile}}\right]=\left[(-\Delta\sigma_i)\cdot\Delta z\cdot L_c\right]$$

**K**: stiffness matrix

$\Delta_z$: distance between two springs or dashpots

$L_c = \pi D/4$: characteristic length

**<u>Assumption</u>: Triaxial conditions for the soil**

From triaxial conditions: $\Delta\sigma_i = \Delta p_i + \frac{2}{3}\Delta q_i$

The unknown volumetric and deviatoric stresses are approximated incrementally with the HCA model:

$$\Delta p_i = K(p_i^0)\,[\Delta\varepsilon_{v_i} - \Delta\varepsilon_{v_i}^{\mathrm{acc}} - \Delta\varepsilon_{v_i}^{\mathrm{pl}}]$$

$$\Delta q_i = 3G(p_i^0)\,[\Delta\varepsilon_{q_i} - \Delta\varepsilon_{q_i}^{\mathrm{acc}} - \Delta\varepsilon_{q_i}^{\mathrm{pl}}]$$

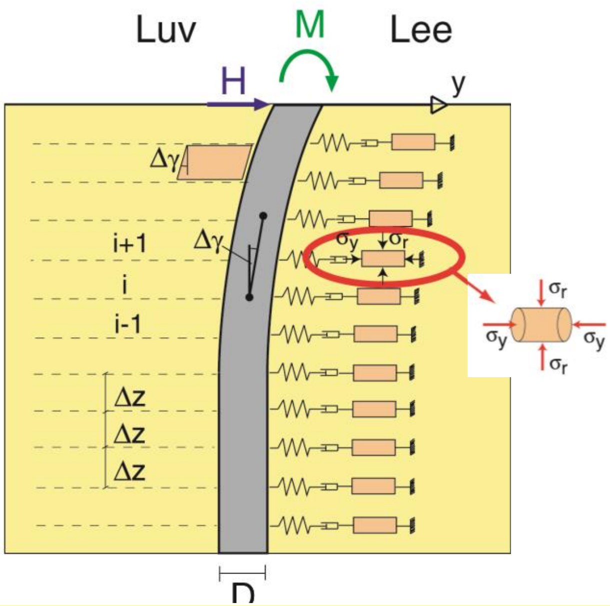


*Triantafyllidis & Chrisopoulos (2016): A model for the behavior of horizontally high-cycle loaded piles. Bautechnik, 93(9): 605-627*

# Engineer-oriented model

## Cyclic loading

$\Delta p_i = K(p_i^0)\ [\Delta\varepsilon_{v_i} - \Delta\varepsilon_{v_i}^{\mathrm{acc}} - \Delta\varepsilon_{v_i}^{\mathrm{pl}}]$ (I)

$\Delta q_i = 3G(p_i^0)\ [\Delta\varepsilon_{q_i} - \Delta\varepsilon_{q_i}^{\mathrm{acc}} - \Delta\varepsilon_{q_i}^{\mathrm{pl}}]$ (II)

Using the HCA flow rule (MCC flow rule) written in terms of Roscoe's invariants and the equation $\Delta\varepsilon_{q_i} = \frac{2}{3}\Delta\gamma_i$ from the triaxial conditions:

$$\Delta\varepsilon_{v_i}^{\mathrm{acc}} = \mathrm{m}_v \cdot \Delta\varepsilon_i^{\mathrm{acc}}, \quad \Delta\varepsilon_{v_i}^{\mathrm{pl}} = \frac{2}{3\sqrt{3}}\mathrm{m}_v \cdot \mathrm{Y} \cdot \Delta\gamma_\iota \ , \quad \Delta\varepsilon_{v_i} = \Delta\varepsilon_{q_i} \cdot \frac{\mathrm{m}_v}{\mathrm{m}_q} = \frac{2}{3}\Delta\gamma_i \cdot \frac{\mathrm{m}_v}{\mathrm{m}_q}$$

$$\Delta\varepsilon_{q_i}^{\mathrm{acc}} = \mathrm{m}_q \cdot \Delta\varepsilon_i^{\mathrm{acc}}, \quad \Delta\varepsilon_{q_i}^{\mathrm{pl}} = \sqrt{\frac{2}{3}} \cdot \mathrm{Y} \cdot \mathrm{m}_q \cdot \Delta\gamma_i^1,$$

Substituting the above equations into (I) and (II) and using the indices $\sqcup^0$ and $\sqcup^1$ for the states at the start and the end of an increment:

$$\Delta p_i^1 = K(p_i^0)\left[\frac{2}{3}\Delta\gamma_i^1 \cdot \frac{\mathrm{m}_v^0}{\mathrm{m}_q^0} - \mathrm{m}_v^0 \cdot \Delta\varepsilon_i^{\mathrm{acc},0} - \mathrm{m}_v^0 \cdot \frac{2}{3\sqrt{3}} \cdot \mathrm{Y}^0 \cdot \Delta\gamma_i^1\right]$$

$$\Delta q_i^1 = 3G(p_i^0)\left[\frac{2}{3}\Delta\gamma_i^1 - \mathrm{m}_q^0 \cdot \Delta\varepsilon_i^{\mathrm{acc},0} - \sqrt{\frac{2}{3}} \cdot \mathrm{Y}^0 \cdot \mathrm{m}_q^0 \cdot \Delta\gamma_i^1\right]$$

# Engineer-oriented model

## Solution process

Using the assumption $\Delta\gamma_i = \frac{\Delta y_{i+1}^{\mathrm{Pile}} - \Delta y_{i-1}^{\mathrm{Pile}}}{2\Delta z}$ the unknown volumetric and deviatoric stresses are written:

$$\Delta p_i^1 = K(p_i^0)\left[\frac{2}{3}\cdot\frac{\Delta y_{i+1}^1 - \Delta y_{i-1}^1}{2\,\Delta z}\cdot\frac{\mathrm{m}_v^0}{\mathrm{m}_q^0} - \mathrm{m}_v^0\cdot\Delta\varepsilon_i^{\mathrm{acc},0} - \mathrm{m}_v^0\cdot\frac{2}{3\sqrt{3}}\cdot \mathrm{Y}^0\cdot\frac{\Delta y_{i+1}^1 - \Delta y_{i-1}^1}{2\,\Delta z}\right]$$

$$\Delta q_i^1 = 3G(p_i^0)\left[\frac{2}{3}\cdot\frac{\Delta y_{i+1}^1 - \Delta y_{i-1}^1}{2\,\Delta z} - \mathrm{m}_q^0\cdot\Delta\varepsilon_i^{\mathrm{acc},0} - \sqrt{\frac{2}{3}}\cdot \mathrm{Y}^0\cdot \mathrm{m}_q^0\cdot\frac{\Delta y_{i+1}^1 - \Delta y_{i-1}^1}{2\,\Delta z}\right]$$

The increment of horizontal displacement $\Delta y_i^{\mathrm{Pile}}$ of the pile is coupled with the unknown increment of stress $\Delta\sigma_i$ in the soil via:

$$[\mathbf{K}]\cdot\left[\Delta y_i^{\mathrm{Pile}}\right] = \left[(-\Delta\sigma_i)\cdot\Delta z\cdot L_c\right] \quad \text{where} \quad \Delta\sigma_i = \Delta p_i + \frac{2}{3}\Delta q_i$$

# Engineer-oriented model

## Solution process

Overall system of equations

$$[\mathbf{G}] \cdot \left[\mathbf{\Delta y_i^{Pile}}\right] = [\mathbf{RHS}]$$

The system of equations is solved for each increment using the program Wolfram Mathematica

$$\underbrace{\begin{bmatrix}
1 & 0 & 0 & 0 & 0 & 0 & 0 & 0 & 0 & 0 & 0 & 0 & 0 & 0 & 0 & 0 & 0 & 0 & 0 & & \cdots & 0 & 0 & 0 & 0 & 0 & 0 & 0 \\
0 & 1 & 0 & 0 & 0 & 0 & 0 & 0 & 0 & 0 & 0 & 0 & 0 & 0 & 0 & 0 & 0 & 0 & 0 & & \cdots & & 0 & 0 & 0 & 0 & 0 & 0 \\
0 & 0 & 1 & 0 & 0 & 0 & 0 & 0 & 0 & 0 & 0 & 0 & 0 & 0 & 0 & 0 & 0 & 0 & 0 & & \cdots & & & 0 & 0 & 0 & 0 & 0 \\
0 & 0 & 0 & 1 & 0 & 0 & 0 & 0 & 0 & 0 & 0 & 0 & 0 & 0 & 0 & 0 & 0 & 0 & 0 & & \cdots & & & & 0 & 0 & 0 & 0 \\
0 & 0 & 0 & 0 & A & B & 0 & 0 & 0 & 0 & -A & B & 0 & 0 & 0 & 0 & 0 & 0 & 0 & & \cdots & & & & & 0 & 0 & 0 \\
0 & 0 & 0 & 0 & B & 2C & 0 & 0 & 0 & 0 & -B & C & 0 & 0 & 0 & 0 & 0 & 0 & 0 & & \cdots & & & & & & 0 & 0 \\
0 & 0 & 0 & 0 & D & 0 & 1 & 0 & 0 & 0 & 0 & 0 & 0 & 0 & 0 & 0 & -D & 0 & 0 & 0 & \cdots & & & & & & & 0 \\
0 & 0 & 0 & 0 & E & 0 & 0 & 1 & 0 & 0 & -E & 0 & 0 & 0 & 0 & 0 & 0 & 0 & 0 & 0 & & & & & & & & \\
0 & 0 & 0 & 0 & F & 0 & 0 & 0 & 1 & 0 & -F & 0 & 0 & 0 & 0 & 0 & 0 & 0 & 0 & 0 & & & & & & & & \\
0 & 0 & 0 & 0 & G & 0 & 0 & 0 & 0 & 1 & -G & 0 & 0 & 0 & 0 & 0 & 0 & 0 & 0 & 0 & & & & & & & & \\
0 & 0 & 0 & 0 & -A & -B & 1 & -1 & 2/3 & -2/3 & 2A & 0 & 0 & 0 & 0 & 0 & -A & B & 0 & 0 & \cdot & & & & & & & \\
0 & 0 & 0 & 0 & B & C & 0 & 0 & 0 & 0 & 0 & 4C & 0 & 0 & 0 & 0 & -B & C & 0 & 0 & \cdot & & & & & & & \\
0 & 0 & 0 & 0 & & & & & & & & & \cdots & & & & & & & & \cdots & & & & & & & \\
\vdots & & & & & & & & & & & & & & & & & & & & \ddots & & & & & & & \vdots \\
0 & \cdot & \cdot & & & & & & & & & & & & & & & & & & & & & & & & & \\
0 & 0 & \cdot & \cdot & & & & & & \cdots & & 0 & 0 & 0 & 0 & 0 & 0 & -D & 0 & 1 & 0 & 0 & 0 & -D & 0 & & & \\
0 & 0 & 0 & \cdot & \cdot & & & & & \cdots & & 0 & 0 & 0 & 0 & 0 & 0 & -E & 0 & 0 & 1 & 0 & 0 & -E & 0 & & & \\
0 & 0 & 0 & 0 & \cdot & \cdot & & & & \cdots & & 0 & 0 & 0 & 0 & 0 & 0 & -F & 0 & 0 & 0 & 1 & 0 & -F & 0 & & & \\
0 & 0 & 0 & 0 & 0 & \cdot & \cdot & & & \cdots & & 0 & 0 & 0 & 0 & 0 & 0 & -G & 0 & 0 & 0 & 0 & 1 & -G & 0 & & & \\
0 & 0 & 0 & 0 & 0 & 0 & \cdot & \cdot & & \cdots & & 0 & 0 & 0 & 0 & 0 & 0 & -A & -B & 1 & -1 & 2/3 & -2/3 & A & -B & & & \\
0 & 0 & 0 & 0 & 0 & 0 & 0 & \cdot & \cdot & \cdots & & 1 & 0 & 0 & 0 & 0 & 0 & -4 & 0 & 0 & 0 & 0 & 0 & 4 & 0 & & &
\end{bmatrix}}_{\mathbf{G}}
\cdot
\underbrace{\begin{bmatrix}
\Delta p^{1\,Lee} \\ \Delta p^{1\,Luv} \\ \Delta q^{1\,Lee} \\ \Delta q^{1\,Luv} \\ \Delta y^{1} \\ \Delta \theta^{1} \\ \Delta p^{2\,Lee} \\ \Delta p^{2\,Luv} \\ \Delta q^{2\,Lee} \\ \Delta q^{2\,Luv} \\ \Delta y^{2} \\ \Delta \theta^{2} \\ \vdots \\ \Delta p^{n\,Lee} \\ \Delta p^{n\,Luv} \\ \Delta q^{n\,Lee} \\ \Delta q^{n\,Luv} \\ \Delta y^{n} \\ \Delta \theta^{n}
\end{bmatrix}}_{\Delta y_{unbekannte}}
=
\underbrace{\begin{bmatrix}
0 \\ 0 \\ 0 \\ 0 \\ 0 \\ 0 \\ -H \\ -I \\ -J \\ -K \\ 0 \\ 0 \\ \vdots \\ 0 \\ 0 \\ -H \\ -I \\ -J \\ -M \\ 0 \\ 0
\end{bmatrix}}_{RHS}$$

$$A = \frac{12EJ}{L^3},\ B = \frac{6EJ}{L^2},\ C = \frac{2EJ}{L},\ D = \frac{2}{3}\frac{m_{vol}{}^{Lee}}{m_q{}^{Lee}}\frac{K(\sigma_{N-1})^{Lee}}{2A_{Fed}},\ E = \frac{2}{3}\frac{m_{vol}{}^{Luv}}{m_q{}^{Luv}}\frac{K(\sigma_{N-1})^{Luv}}{A_{Fed}},\ F = \frac{2G(\sigma_{N-1})^{Lee}}{A_{Fed}},$$

$$G = \frac{2G(\sigma_{N-1})^{Luv}}{A_{Fed}},\ H = K(\sigma_{N-1})^{Lee}\cdot\left(\Delta\varepsilon_N{}^{acc\,Lee} + \Delta\varepsilon_N{}^{pl\,Lee}\right),\ I = K(\sigma_{N-1})^{Luv}\cdot\left(\Delta\varepsilon_N{}^{acc\,Luv} + \Delta\varepsilon_N{}^{pl\,Luv}\right),$$

$$J = 3G(\sigma_{N-1})^{Lee}\cdot m_q{}^{Lee}\left(\Delta\varepsilon_N{}^{acc\,Lee} + \Delta\varepsilon_N{}^{pl\,Lee}\right),\ M = 3G(\sigma_{N-1})^{Luv}\cdot m_q{}^{Luv}\left(\Delta\varepsilon_N{}^{acc\,Luv} + \Delta\varepsilon_N{}^{pl\,Luv}\right)$$

# Engineer-oriented model

## Results and validation

Comparison of the pile deflections of an OWPP monopile foundation after $10^5$ cycles

<u>Parameters</u>: Pile diameter 5 m, depth of embedding 30 m, initial relative density of the soil $I_{D0}$ =0,6 and lever arm h=M/V = 20 m

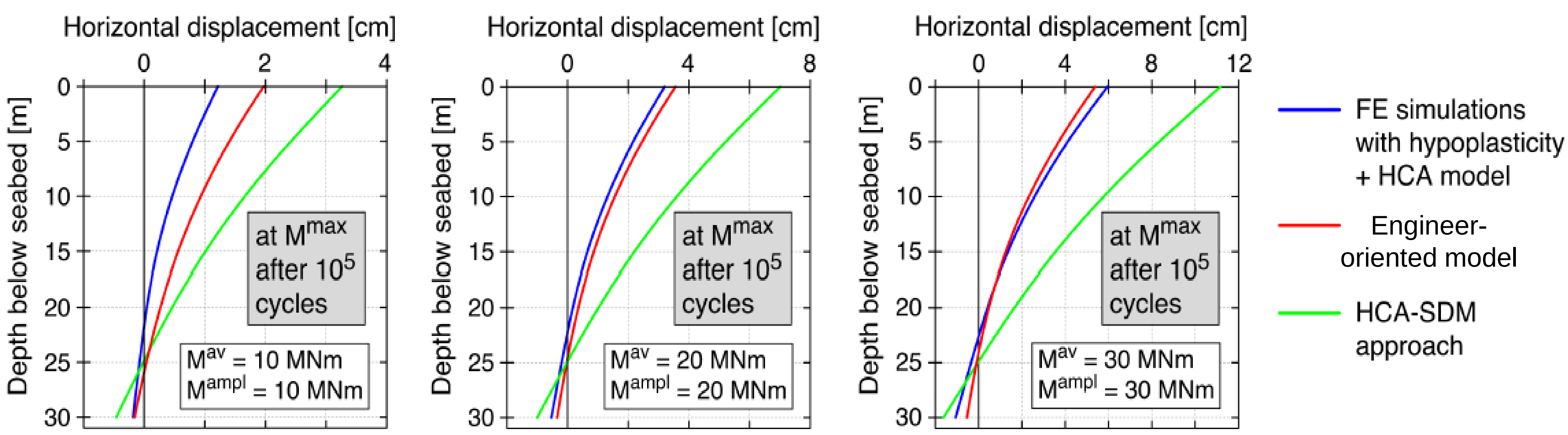


The deflection curves obtained from the engineer oriented model lie close to the results from the full FE simulations with the HCA model.

*Triantafyllidis & Chrisopoulos (2016): A model for the behavior of horizontally high-cycle loaded piles. Bautechnik, 93(9): 605-627*

# iii. Estimation of the dynamic foundation-subsoil interaction of a wind turbine

# Dynamic Soil-Structure interaction

- Determination of the complex dynamic stiffness of the circular foundation of the WT due to an impulse
- Analytical solutions (Triantafyllidis et al. 1987)

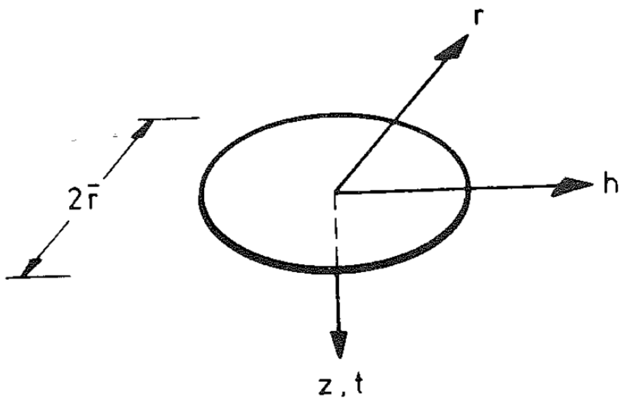


- horizontal translation *h*
- vertical translation *z*
- rotation about *r* (rocking)
- rotation about *z* (torsion)

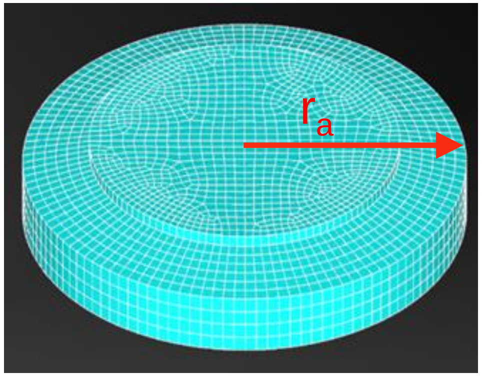


For translation:

$$Re(F_j) = u_j \underbrace{\boxed{G\, r_a\, K_{jj}}}_{k_{jj}}$$

$$Im(F_j) = \omega\, u_j \underbrace{\boxed{r_a^2 \sqrt{G\, \rho}\, C_{jj}}}_{c_{jj}}$$

For rotation:

$$Re(M_j) = \hat{u}_j \underbrace{\boxed{G\, r_a^3\, K_{jj}}}_{k_{\hat{j}\hat{j}}}$$

$$Im(M_j) = \omega\, \hat{u}_j \underbrace{\boxed{r_a^4 \sqrt{G\, \rho}\, C_{jj}}}_{c_{\hat{j}\hat{j}}}$$

$K_{jj}$ : Dimensionless spring parameter

$C_{jj}$ : Dimensionless damper parameter

$r_a$ : Radius of the circular foundation

G : Shear stiffness

ρ : Density

$v_s$ : Shear wave velocity

# Dynamic Soil-Structure interaction

## Calculation of the dimensionless spring $K_{jj}$ and damper parameter $C_{jj}$

$$K_{jj} = C_0 + C_1 \cdot \alpha_0 + C_2 \cdot \alpha_0{}^2 + C_3 \cdot \alpha_0{}^3 + \ldots\ldots + C_6 \cdot \alpha_0{}^6 = \sum_{i=0}^{6} C_i \cdot \alpha_0{}^i$$

$$C_{jj} = C_0 + C_1 \cdot \alpha_0 + C_2 \cdot \alpha_0{}^2 + C_3 \cdot \alpha_0{}^3 + \ldots\ldots + C_6 \cdot \alpha_0{}^6 = \sum_{i=0}^{6} C_i \cdot \alpha_0{}^i$$

with the dimensionless frequency $\alpha_0 = \frac{\omega\, r_a}{v_s}$ and the coefficients $C_0 \ldots C_6$ (from Tables)

| | Kzz | | | Czz | | |
|---|---|---|---|---|---|---|
| NY | 0.25 | 0.33 | 0.40 | 0.25 | 0.33 | 0.40 |
| C0 | -0.66796+1 | -0.61402+1 | -0.54920+1 | -0.52469+1 | -0.48135+1 | -0.44293+1 |
| C1 | -0.11174+1 | +0.83234-1 | -0.48845+0 | -0.42338-1 | -0.36151-1 | -0.26038-1 |
| C2 | +0.42391+1 | +0.30600+0 | +0.10339+1 | -0.15837+0 | -0.12768+0 | -0.98526-1 |
| C3 | -0.42496+1 | +0.23483+0 | -0.22400+0 | | | |
| C4 | +0.24668+1 | -0.78015-1 | | | | |
| C5 | -0.67817+0 | | | | | |
| C6 | +0.68804-1 | | | | | |

Table 2. Stiffness Functions Kzz (Real Part) and Czz (Imaginary Part) of Circular Foundation for Vertical Translation z

# Dynamic Soil-Structure interaction

## Calculation of the dimensionless spring $K_{jj}$ and damper parameter $C_{jj}$

$$K_{jj} = C_0 + C_1 \cdot \alpha_0 + C_2 \cdot \alpha_0{}^2 + C_3 \cdot \alpha_0{}^3 + \ldots\ldots + C_6 \cdot \alpha_0{}^6 = \sum_{i=0}^{6} C_i \cdot \alpha_0{}^i$$

$$C_{jj} = C_0 + C_1 \cdot \alpha_0 + C_2 \cdot \alpha_0{}^2 + C_3 \cdot \alpha_0{}^3 + \ldots\ldots + C_6 \cdot \alpha_0{}^6 = \sum_{i=0}^{6} C_i \cdot \alpha_0{}^i$$

with the dimensionless frequency $\alpha_0 = \frac{\omega\, r_a}{v_s}$ and the coefficients $C_0 \ldots C_6$ (from Tables)

| | Krr | | | Crr | | |
|---|---|---|---|---|---|---|
| NY | 0.25 | 0.33 | 0.40 | 0.25 | 0.33 | 0.40 |
| C0 | -0.45303+1 | -0.41889+1 | -0.38228+1 | -0.17387-1 | -0.24865-1 | -0.31811-1 |
| C1 | +0.27100+0 | +0.56923+0 | +0.47386+0 | +0.28649+0 | +0.27256+0 | +0.15229+0 |
| C2 | +0.79905+0 | +0.17266+0 | +0.17872+0 | -0.20349+1 | -0.18426+1 | -0.12575+1 |
| C3 | -0.36608+0 | -0.45346-1 | -0.48259-1 | +0.18237+1 | +0.16423+1 | +0.91185+0 |
| C4 | +0.52855-1 | | | -0.76877+0 | -0.69643+0 | -0.27172+0 |
| C5 | | | | +0.15980+0 | +0.14742+0 | +0.29665-1 |
| C6 | | | | -0.13167-1 | -0.12535-1 | |

Table 3. Stiffness Functions Krr (Real Part) and Crr (Imaginary Part) of Circular Foundation for Rotation r (Rocking)

# Dynamic Soil-Structure interaction

Calculation of the complex dynamic stiffness ($k_{jj}$ und $c_{jj}$)

**Example (vertical translation):**

Parameters of soil (limestone)

$\rho$ = 2,6 tn/m³, G = 1,26 * 10⁴ MN/m², $v_s$ = 2200 m/s, $r_a$ = 9,8 m, v = 0,25

for $f = 5$ Hz $\longrightarrow$ $\omega = 2\pi f = 31{,}42$ rad/s $\longrightarrow$ $\alpha_0 = \frac{\omega\, r_a}{v_s} = \frac{12{,}57 * 9{,}9}{2200} = 0{,}14$

$$K_{zz} = \sum_{i=0}^{6} C_i \cdot {\alpha_0}^i = -6{,}67 - 1{,}12 \cdot 0{,}14 + 4{,}24 \cdot 0{,}14^2 - 4{,}25 \cdot 0{,}14^3 + \cdots + 0{,}069 \cdot 0{,}14^6 = -6{,}76$$

$$C_{zz} = \sum_{i=0}^{6} C_i \cdot {\alpha_0}^i = -5{,}25 - 0{,}042 \cdot 0{,}14 - 0{,}158 \cdot 0{,}14^2 = -5{,}26$$

$$\longrightarrow k_{zz} = G\, r_a\, K_{zz} = -1{,}26 \cdot 10^4 \cdot 9{,}8 \cdot 6{,}76 = -8{,}35 \cdot 10^5 \text{ MN/m}$$

$$\longrightarrow c_{zz} = r_a^2 \sqrt{G\,\rho}\, C_{zz} = -9{,}8^2 \cdot \sqrt{1{,}26 \cdot 10^4 \cdot 0{,}0026} \cdot 5{,}26 = -2{,}89 \cdot 10^3 \text{ MN·s/m}$$

$$Re(F_j) = u_j \underbrace{\boxed{G\, r_a\, K_{zz}}}_{k_{zz}} \qquad Im(F_j) = \omega\, u_j \underbrace{\boxed{r_a^2 \sqrt{G\,\rho}\, C_{zz}}}_{c_{zz}}$$

DAADDeutscher Akademischer Austausch Dienst
German Academic Exchange Service

KIT Karlsruhe Institute of Technology

UNIVERSITY OF PATRAS

# Dynamic Soil-Structure interaction

Calculation of the complex dynamic stiffness ($k_{jj}$ und $c_{jj}$)

**Example (vertical translation):**

Parameters of soil (limestone)

$\rho$ = 2,6 tn/m$^3$, G = 1,26 * 10$^4$ MN/m$^2$, $v_s$ = 2200 m/s, $r_a$ = 9,8 m, v = 0,25

for varying frequencies: $k_{zz}$ (f), $c_{zz}$ (f)

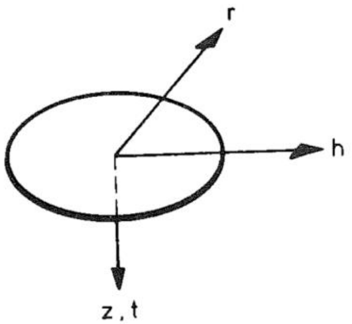


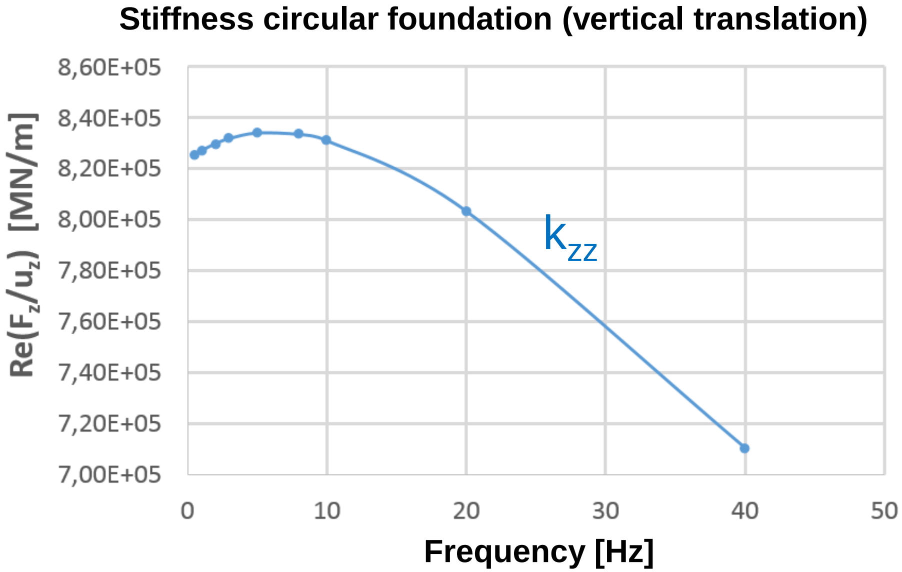


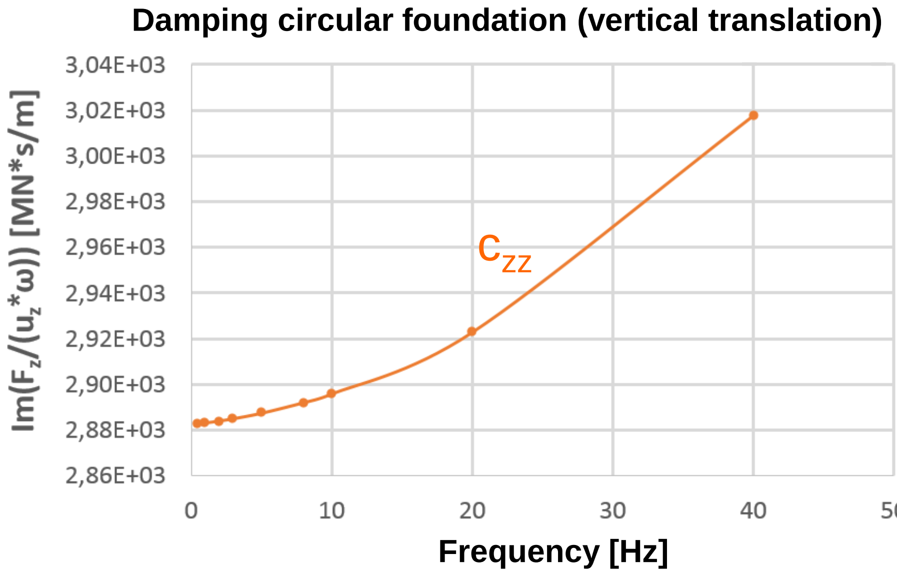

# Dynamic Soil-Structure interaction

Calculation of the complex dynamic stiffness ($k_{\hat{jj}}$ und $c_{\hat{jj}}$)

**Example (rotation about r):**

Parameters of soil (limestone)

$\rho$ = 2,6 tn/m$^3$, G = 1,26 * 10$^4$ MN/m$^2$, $v_s$ = 2200 m/s, $r_a$ = 9,8 m, v = 0,25

for $f = 5\ \mathrm{Hz} \longrightarrow \omega = 2\pi f = 31{,}42$ rad/s $\longrightarrow \alpha_0 = \frac{\omega\, r_a}{v_s} = \frac{12{,}57*9{,}9}{2200} = 0{,}14$

$K_{\hat{zz}} = \sum_{i=0}^{6} C_i \cdot \alpha_0{}^i = -4{,}53 + 0{,}27 \cdot 0{,}14 + 0{,}80 \cdot 0{,}14^2 - 0{,}37 \cdot 0{,}14^3 + 0{,}052 \cdot 0{,}14^4 = -4{,}47$

$C_{\hat{zz}} = \sum_{i=0}^{6} C_i \cdot \alpha_0{}^i = -0{,}017 + 0{,}286 \cdot 0{,}14 - 2{,}03 \cdot 0{,}14^2 + 1{,}82 \cdot 0{,}14^3 + \cdots -0{,}01 \cdot 0{,}14^6 = -0{,}012$

$\longrightarrow k_{\hat{rr}} = G\, r_a^3\, K_{\hat{rr}} = -1{,}26 \cdot 10^4 \cdot 9{,}8^3 \cdot 4{,}47 = -5{,}3 \cdot 10^7$ MN/m

$\longrightarrow c_{\hat{rr}} = r_a^4 \sqrt{G\,\rho}\, C_{\hat{rr}} = -9{,}8^4 \cdot \sqrt{1{,}26 \cdot 10^4 \cdot 0{,}0026} \cdot 0{,}012 = -6{,}3 \cdot 10^2$ MN·s/m

$\mathrm{Re}(M_j) = \hat{u}_j \underbrace{\boxed{G\, r_a^3\, K_{\hat{rr}}}}_{k_{\hat{rr}}} \qquad \mathrm{Im}(M_j) = \omega\, \hat{u}_j \underbrace{\boxed{r_a^4 \sqrt{G\,\rho}\, C_{\hat{rr}}}}_{c_{\hat{rr}}}$



Deutscher Akademischer Austausch Dienst
German Academic Exchange Service
Karlsruhe Institute of Technology
UNIVERSITY OF PATRAS

# Dynamic Soil-Structure interaction

Calculation of the complex dynamic stiffness ($k_{\hat{jj}}$ und $c_{\hat{jj}}$)

**Example (rotation about r):**

Parameters of soil (limestone)

ρ = 2,6 tn/m³, G = 1,26 * 10⁴ MN/m², $v_s$ = 2200 m/s, $r_a$ = 9,8 m, v = 0,25

for varying frequencies: $k_{\hat{rr}}$ (f), $c_{\hat{rr}}$ (f)

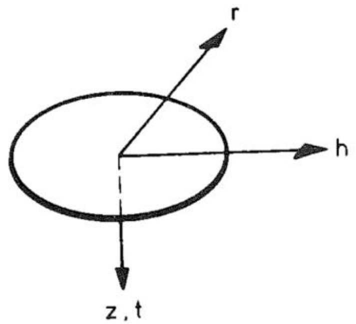


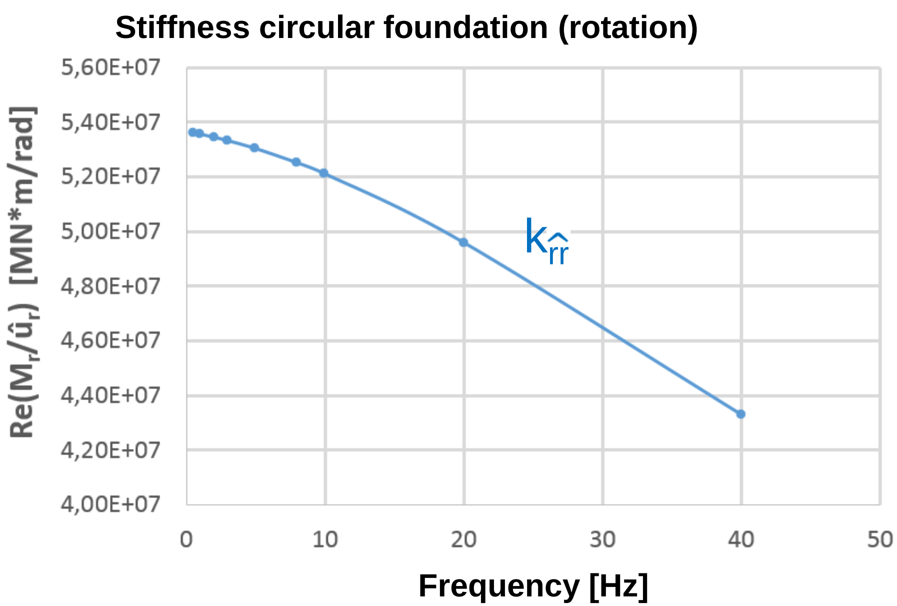


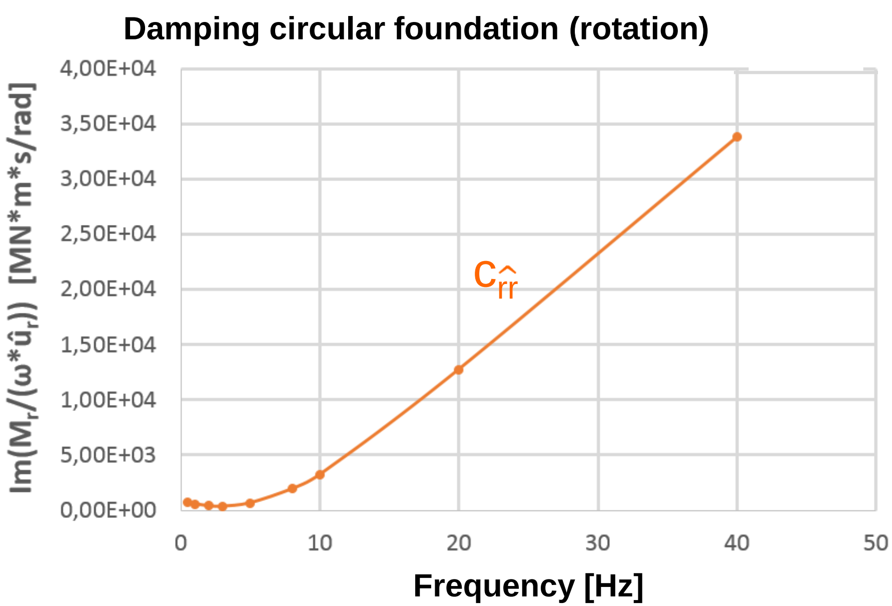

**Thank you for your attention!**